Available online at www.sciencedirect.com
SCIENCE DIRECT®
Journal of Organometallic Chemistry 690 (2005) 5264–5281
Journal of Organometallic Chemistry
www.elsevier.com/locate/jorganchem

Diphenylphosphino(phenyl pyridin-2-yl methylene)amine palladium(II) complexes: Chemoselective alkene hydrocarboxylation initiators

Philip W. Dyer [a,b,*], John Fawcett [b], Martin J. Hanton [b,1]

[a] Department of Chemistry, University of Durham, South Road, Durham DH1 3LE, UK
[b] Department of Chemistry, University of Leicester, University Road, Leicester LE1 7RH, UK

Received 1 February 2005; received in revised form 18 April 2005; accepted 20 April 2005
Available online 16 June 2005

Abstract

The heteroditopic, P–N-chelating ligand diphenylphosphino(phenyl pyridin-2-yl methylene)amine (**1**) has been synthesised via a simple 'one-pot' procedure and its donor characteristics assessed. The neutral [MX(Y)(**1**-κ^2-P–N)] (**3**, M = Rh, X = Cl, Y = CO; **4**, M = Pd, X = Y = Cl; **5**, M = Pd, X = Cl, Y = Me; **6**, M = Pt, X = Y = Cl; **7**, M = Pt, X = Cl, Y = Me; **8**, M = Pt, X = Y = Me) and cationic [Pd(Me)(MeCN)(**1**-κ^2-P–N)][Z] (**9**, Z = B{3,5-$(CF_3)_2$-C_6H_3}4; **10**, Z = PF_6) complexes of **1** have been prepared and characterised. The solid-state structures of complexes **3**, **4**, **6** and **7** have been established by X-ray crystallography. Reactions of [PdCl(Me)(**1**-κ^2-P–N)] towards CO and ^{t}BuNC have been investigated, affording the corresponding η^1-acyl (**12**) and -iminoacyl (**14**) complexes, respectively. Similar insertion chemistry is observed for the cationic derivative **9**. Treatment of the acyl complex **12** with ethene at elevated pressure establishes an equilibrium between the starting material and the product resulting from insertion, **13**. Under catalytic conditions, combination of palladium(II) with **1** in MeOH affords a selective initiator for the formation of 4-oxohexanoic acid methyl ester (**15**) from CO/ethene (38 bar, 90 °C).

Keywords: P–N ligands; Palladium; Polyketone; Hydrocarboxylation

1. Introduction

There is continued interest in the application of heteroditopic ligands to a variety of catalytic processes, with bidentate P–N derivatives having been the focus of particular attention [1]. The asymmetry present in systems of this type offers a degree of selectivity in reactions occurring at the metal centre, due to the electronic and steric disparity between the two different donor groups. Furthermore, they provide a means of introducing a wide range of variously substituted donor units into the coordination sphere of metals.

One area in which P–N ligands have received comparatively little attention is that of the production of low molecular weight oxygenates from CO and alkenes via co-oligomerisation, despite the extensive application of both P–P and N–N bidentate ligands [2–5]. Such reactions are of significant industrial interest. Since they can be tuned to provide routes to carboxylic acids, diacids, polyketones and esters, all valuable organic building blocks. In particular, shorter chain alkene–CO oligomers (oxygenates) have found widespread use as solvents, in part because of their low cost, but also as a result of their low environmental impact [3].

For a number of years we have been interested in the preparation of chelating phosphorus–nitrogen scaffolds

* Corresponding author. Tel.: +44 191 334 2150; fax: +44 191 384 4737.
E-mail address: p.w.dyer@durham.ac.uk (P.W. Dyer).
[1] Current address: Sasol Technology UK Research Laboratory, Purdie Building, North Haugh, St. Andrews, Fife KY16 9ST, UK.

0022-328X/$ - see front matter © 2005 Elsevier B.V. All rights reserved.
doi:10.1016/j.jorganchem.2005.04.032

and have focussed our attention upon systems that could be prepared through the formation of a P–N bond [6,7]. This methodology is attractive not only because such reactions are generally easily achieved, but also because the resulting aminophosphine component is an electronically and sterically flexible donor moiety in its own right [8–10].

Here, we report the synthesis and coordination chemistry of readily prepared diphenylphosphino(phenyl pyridin-2-yl methylene)amine, an attractive ligand that combines an aminophosphine fragment in a potentially 6-membered chelate-forming system. Emphasis is placed on the preparation, characterisation and reactivity of the palladium(II) complexes of this ligand, prior to demonstrating their utility for the selective oligomerisation of CO/C_2H_4. It was of particular interest to probe the reactivity of the palladium methyl complex **5**, since the insertion of carbon monoxide into palladium–alkyl bonds is of considerable relevance in a range of catalytic processes [11–13,23].

2. Results and discussion

2.1. Synthesis of ligand *1*

The heteroditopic P–N ligand **1** is prepared in two steps using a straightforward 'one-pot' procedure starting from 2-cyanopyridine (Scheme 1) and isolated following purification by Soxhlet extraction with hexane (45% yield). Air and moisture sensitive compound **1** is stable for several hours as a dry solid under air, but for only minutes in solution if non-dried solvents are employed.

The somewhat low yield of **1** is presumed to result from competitive ring deprotonation of 2-cyanopyridine by PhLi. In an attempt to alleviate this problem, less basic PhMgBr was used in the place of the organolithium reagent. However, in this case only a trace of **1** was obtained according to the $^{31}P\{^1H\}$ NMR spectrum of the crude reaction mixture.

The $^{31}P\{^1H\}$ NMR spectrum of **1** shows a single sharp resonance at a chemical shift typical of a diarylaminophosphine, +41.9 ppm $\{CD_2Cl_2\}$ [8,14]. In the $^{13}C\{^1H\}$ NMR spectrum, a signal readily attributable to the imine carbon (C^6) is observed at a characteristic chemical shift (δ: 171.8), exhibiting a small two-bond coupling to P ($^2J_{PC}$ = 7 Hz) [6,15]. Given the relative magnitudes of the three-bond couplings to phosphorus exhibited by C^5 ($^3J_{PC}$ = 6 Hz) and C^7 ($^3J_{PC}$ = 11 Hz), analysis by a modified Karplus relationship suggests that the imine bond adopts a Z configuration with respect to the pyridyl ring [16].

2.2. Assessment of the donor characteristics of the P-component of ligand *1*

Iminopyridyl phosphine **1** reacts cleanly and quantitatively with elemental selenium upon sonication to afford the corresponding mono-selenide **2** [$^{31}P\{^1H\}$ NMR δ: +42.6 ($^1J_{SeP}$ = 769 Hz)] (Scheme 2). This derivative can be used to assess the donor characteristics of the P-component of **1**, since there exists a well-established correlation between the magnitude of $^1J_{PSe}$ coupling constants and the basicity of phosphines: the greater the value of $^1J_{PSe}$, the greater the *s*-character of the P lone pair and hence the poorer its donating ability [17]. The magnitude of $^1J_{PSe}$ obtained for **2** is consistent with the P-component of **1** being a comparatively poor σ-donor (comparable with other diarylaminophosphines) [8]. This is presumed to be a consequence of both partial delocalisation of the P lone pair into the conjugated π-system of the ligand backbone and the electronegativity of nitrogen.

The rhodium carbonyl chloride complex [RhCl(CO)(**1**-κ^2-P–N)] (**3**) is formed quantitatively upon treating a $CDCl_3$ solution of **1** with 0.5 equivalents of $[RhCl(CO)_2]_2$ under a CO atmosphere (Scheme 2). The $^{31}P\{^1H\}$ NMR spectrum of **3** [δ: +84.5 ($^1J_{RhP}$ = 167 Hz)] reveals a doublet with a downfield coordination chemical shift ($\Delta\delta$) of ~43 ppm compared to unbound **1**. The magnitude of the $^1J_{RhP}$ coupling constant is indicative of the geometry at Rh being CO *cis* to P as would be expected on thermodynamic grounds, and is comparable in size to that observed for similar systems [18–20]. The value of $^1J_{RhP}$ is consistent with the P-component of **1** being a relatively poor donor (vide supra). IR spectroscopy shows a single strong carbonyl stretch at 2010 cm^{-1}. This value is consistent with that determined for a recently reported, related P–N chelate, possessing a pyridyl moiety and an aminophosphine bound to rhodium [21]. Although the use of the carbonyl stretching frequency of *trans*-[RhCl(CO)L_2] complexes as a measure of the donor behaviour of L is well-established [8,22], the relationship for *cis*-chelating bidentate ligands is less clear. However, the value determined here for **3** is

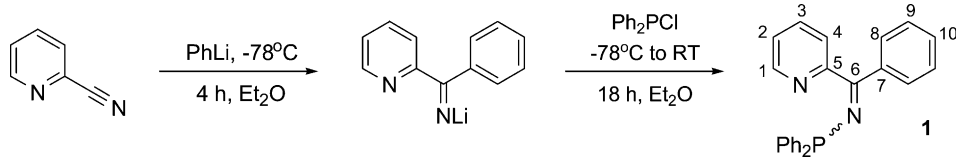

Scheme 1. The synthesis of ligand **1** (with spectroscopic numbering scheme).

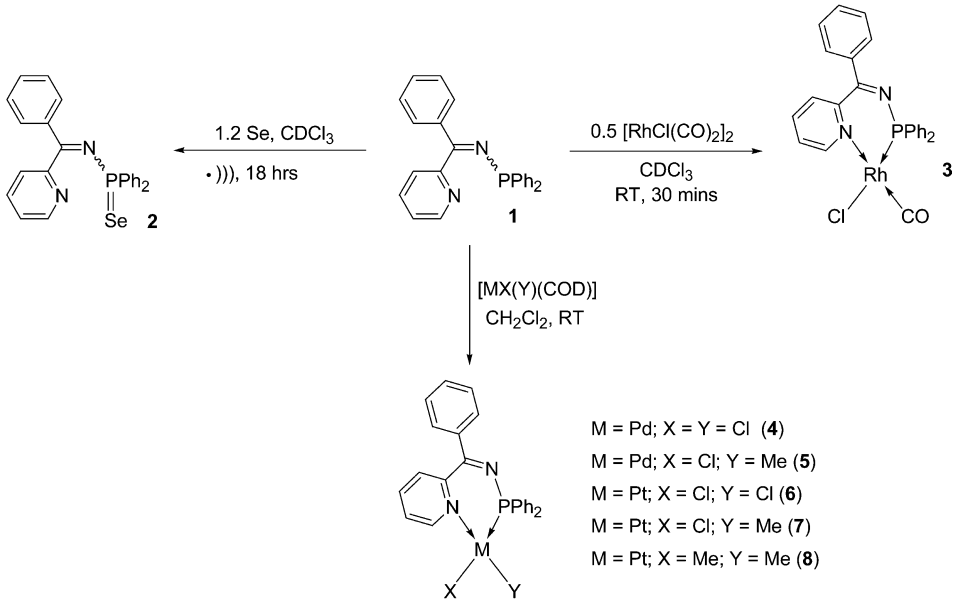

Scheme 2. Reactions of ligand **1** with selenium and complexes of Rh(I), Pd(II) and Pt(II).

still indicative of poor σ-donor/high π-acceptor character, and is in line with the deduction made from the $^1J_{PSe}$ coupling constant (vide supra).

2.3. Synthesis of neutral palladium(II) and neutral platinum(II) complexes of ligand *1*

Due to their relevance in carbon monoxide/alkene copolymerisation, palladium(II) complexes of ligand **1** were attractive targets [23]. The complexes [$PdCl_2$(**1**-κ^2-P–N)] (**4**) and [PdCl(Me)(**1**-κ^2-P–N)] (**5**) were prepared by reaction of a slight excess of **1** with [$PdCl_2$(COD)] and [PdCl(Me)(COD)], respectively, in CH_2Cl_2 at RT and isolated in excellent yields of 94% and 87% (Scheme 2). Using analogous reaction conditions, the related platinum(II) complexes [$PtCl_2$(**1**-κ^2-P–N)] (**6**), [PtCl(Me)(**1**-κ^2-P–N)] (**7**), [$PtMe_2$(**1**-κ^2-P–N)] (**8**) were all obtained from the reaction of **1** with the appropriate [Pt(X)(Y)(COD)] precursor in excellent yields of ca. 90% (Scheme 2).

2.4. NMR characterisation of neutral palladium(II) and platinum(II) complexes of ligand *1*

Each of the complexes **4**–**8** shows a single resonance by $^{31}P\{^1H\}$ NMR spectroscopy at a shift indicative of a metal-coordinated diarylaminophosphine, with a downfield coordination chemical shift (Δδ), except for **6**, where Δδ = −2.4 ppm (Table 1) [8,24]. For complexes **6**–**8**, the $^{31}P\{^1H\}$ NMR spectral data reveal the expected trend in the magnitudes of the $^1J_{PtP}$ coupling constants, the smallest value being observed for

Table 1
Selected NMR spectroscopic data for ligand **1** and complexes **3**–**10**

Compound	δ $^{31}P\{^1H\}$[a]	δ ^1H	δ $^{13}C\{^1H\}$	
		M–C*H*$_3$	C^6=N	M–*C*H$_3$
1	+41.9	–	171.8 ($^2J_{PC}$ 7 Hz)[a]	–
3	+84.5 ($^1J_{RhP}$ 167 Hz)	–	176.5[b]	–
4	+66.8	–	181.6[a] ($^2J_{PC}$ 5 Hz)	–
5	+72.9	0.54[b] ($^3J_{PH}$ 3.2 Hz)	177.3[b] ($^2J_{PC}$ 4 Hz)	−0.7[b]
6	+39.5 ($^1J_{PtP}$ 3806 Hz)	–	180.7[b] ($^2J_{PC}$ 5 Hz)	–
7	+46.9 ($^1J_{PtP}$ 4800 Hz)	0.53[b] ($^3J_{PH}$ 3.7, $^2J_{PtH}$ 79.9 Hz)	177.4[b] ($^2J_{PC}$ 5 Hz)	−16.7 ($^2J_{PC}$ 5, $^1J_{PtC}$ 677 Hz)[b,c]
8	+65.3 ($^1J_{PtP}$ 1259 Hz)	0.53[b] ($^3J_{PH}$ 7.9, $^2J_{PtH}$ 90.6 Hz) 0.77[b] ($^3J_{PH}$ 7.9, $^2J_{PtH}$ 65.4 Hz)	175.0[b] ($^3J_{PtC}$ 27 Hz)	10.9[b,d] ($^2J_{PC}$ 111, $^1J_{PtC}$ 340 Hz) −21.6[b,c] ($^2J_{PC}$ 4, $^1J_{PtC}$ 759 Hz)
9	+73.7[b]	0.35[b] ($^3J_{PH}$ 2.3 Hz)	178.5[b] ($^2J_{PC}$ 6 Hz)	0.7
10	+73.4 ($v_{1/2}$ = 14.3 Hz)[b,e]	0.38[b] (br, $v_{1/2}$ = 4.2 Hz)	178.1[b] ($^2J_{PC}$ 6 Hz)	1.2

[a] Measured in CD_2Cl_2 at 300 K.
[b] Measured in $CDCl_3$ at 300 K.
[c] Me *cis* P.
[d] Me *trans* P.
[e] Cation only.

dimethyl complex **8** ($^1J_{PtP}$ = 1259 Hz) in which there is a strongly *trans*-influencing methyl ligand *trans* to the P-donor fragment [25].

The ^{1}H NMR spectra of complexes **4**–**8** are broadly similar to those of **1**, but reveal downfield values of $\Delta\delta$ (≈1 ppm) for the C^1–*H* resonances, which also exhibit four-bond coupling to P ($^4J_{PH} \approx 1$ Hz), consistent with bidentate P–N binding. Additionally, the C^1–*H* resonances for complexes **7** and **8** also show a $^3J_{PtH}$ coupling of 15.4 and 21.9 Hz, respectively. Discrimination of the *cis*- and *trans*-methyl resonances of **8** was achieved through a ^{1}H NOESY NMR experiment; assignment based solely on coupling constants is unreliable [28]. By ^{13}C{^{1}H} NMR spectroscopy, a downfield shift of ca. 5–10 ppm for the imine carbon C^6, compared to unbound **1**, was observed for each of the complexes.

The spectroscopic data obtained for complex **5** confirm its regioselective formation, a single resonance being observed by ^{31}P {^{1}H} NMR spectroscopy {δ: +72.9}, with one Pd–*CH*$_3$ resonance appearing in both the ^{1}H and ^{13}C NMR spectra {^{1}H, δ: 0.54 ($^3J_{PH}$ = 3.2 Hz); ^{13}C, δ: −0.71}. These data are consistent with the formation of the thermodynamic isomer in which the methyl group occupies a position *cis* to the P donor fragment, the small coupling observed being comparable to that observed in other similar systems [26–28].

2.5. X-ray crystallographic investigation of complexes of ligand *1*

Crystals suitable for study by X-ray diffraction were obtained for **3**, **4**, **6** and **7** by slow diffusion of hexane into a chlorocarbon solution of the appropriate complex. The molecular structures of **3**, **4**, **6** and **7** are presented in Figs. 1–4, respectively. Tables 2 and 3 list selected bond distances and bond angles and Table 5 gives selected crystal data and refinement details.

The gross molecular structures of complexes **3**, **4**, **6** and **7** confirm both the square planar geometry about the metal centres and the bidentate P–N binding mode of ligand **1**. In each case, the chelate ring adopts a 'distorted-boat' conformation, which presumably results from the inclusion of the aromatic ring and the imine double bond within the chelate that resist being twisted out-of-plane. The imine carbon C^6 is essentially planar in each structure, as expected. The plane of the pyridyl ring is twisted out of the square coordination plane about the metal {angle between planes in the range 25.6 (**7**) to 39.6° (**6**)} for all four complexes. This reflects a degree of flexibility associated with the P–N chelate ring, something further exemplified by the variation of the ligand bite angle with values ranging from 82.71(4) (**3**) to 85.29(8)° (**7**).

The heteroditopic nature of ligand **1** influences both the synthesis and the resulting structures of its complexes, as a consequence of the greater *trans*-influence

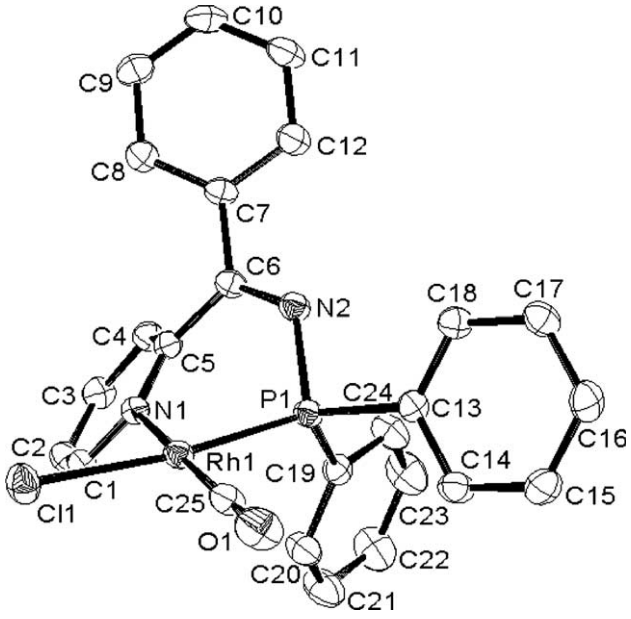

Fig. 1. Thermal ellipsoid plot (50% probability) of [RhCl(CO)(**1**-κ^2-P–N)] (**3**), hydrogen atoms and molecule of $CDCl_3$ omitted for clarity.

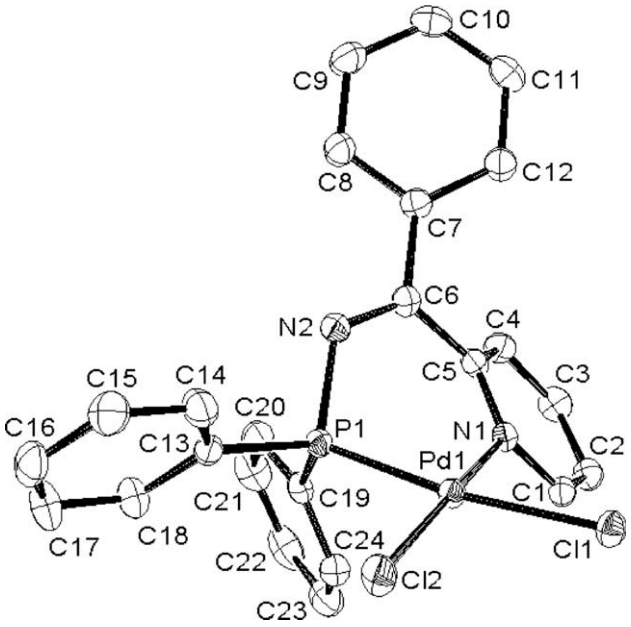

Fig. 2. Thermal ellipsoid plot (50% probability) of **4**, hydrogen atoms and molecule of CD_2Cl_2 omitted for clarity.

of the P moiety compared to that of the pyridyl N-atom [29]. For complex **4**, a pronounced elongation (∼0.11 Å) of the Pd(1)–Cl(1) bond compared to the Pd(1)–Cl(2) bond is observed. A similar situation occurs for complex **6**, where two inequivalent Pt(1)–Cl bond distances are identified that differ by ∼0.08 Å.

The molecular structures of the rhodium complex **3** and the platinum complex **7** are entirely consistent with those inferred from NMR spectroscopy (vide infra). They confirm that **3** adopts the thermodynamic isomer

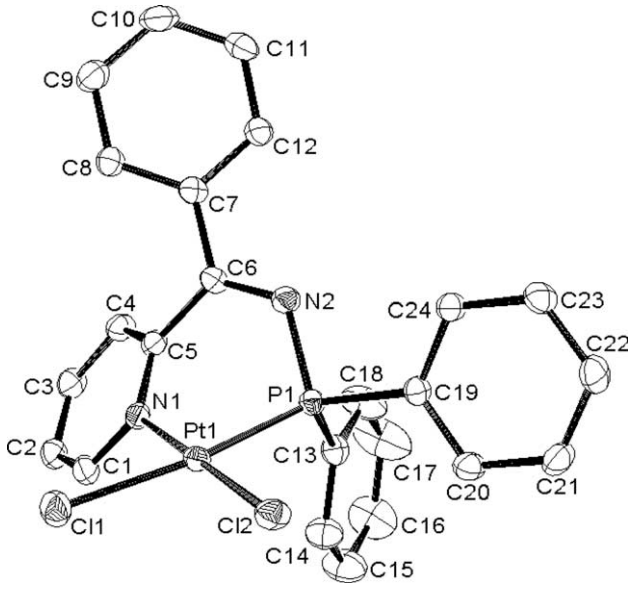

Fig. 3. Thermal ellipsoid plot (50% probability) of **6**, hydrogen atoms and molecule of CH_2Cl_2 omitted for clarity.

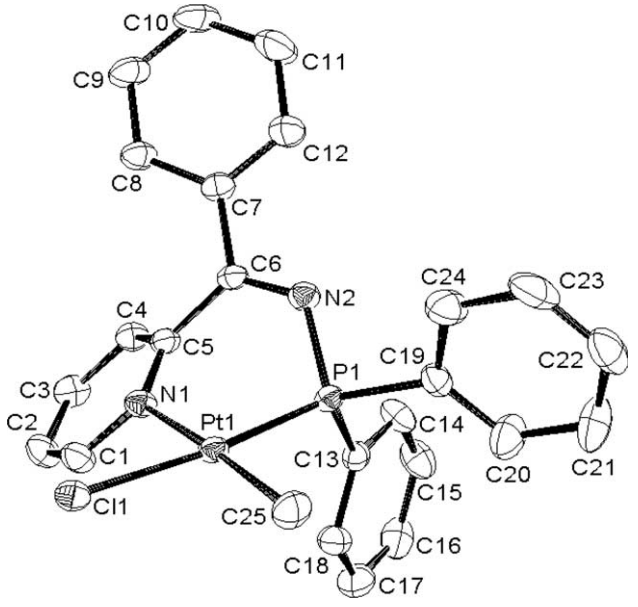

Fig. 4. Thermal ellipsoid plot (50% probability) of **7**, hydrogen atoms omitted for clarity.

with the CO ligand located *cis* to the P-donor fragment, and for complex **7** that the pyridyl ring adopts a position *trans* to the methyl group, in accord with the relative *trans*-influences of each of the ligands. Furthermore, the difference in the Pt(1)–N(1) bond distances {**6**: 2.0564(4) Å; **7**: 2.1643(9) Å}, clearly reflects the greater *trans*-influence of a methyl versus a chloride ligand [18].

The P(1)–N(2) bond distances for the complexes **3**, **4**, **6** and **7** lie in the range 1.684(4)–1.7018(16) Å. Although shorter than the values normally attributed to P–N single bonds, the possibility of a degree of phosphorus–nitrogen multiple bond character can be ruled out since the orientation of the imine N atom precludes N → P retro-donation [30]. Indeed, this metric parameter is

Table 2
Selected bond lengths and angles for [RhCl(CO)(**1**-κ^2-P–N)] (**3**) and [$PdCl_2$(**1**-κ^2-P–N)] (**4**)

Complex **3**		Complex **4**	
Bond distances (Å)			
Rh(1)–C(25)	1.814(2)	Pd(1)–N(1)	2.0610(14)
Rh(1)–N(1)	2.1475(16)	Pd(1)–P(1)	2.1983(5)
Rh(1)–P(1)	2.1905(5)	Pd(1)–Cl(1)	2.3813(4)
Rh(1)–Cl(1)	2.3802(5)	Pd(1)–Cl(2)	2.2728(5)
O(1)–C(25)	1.145(3)	P(1)–N(2)	1.6984(15)
P(1)–N(2)	1.7018(16)	P(1)–C(13)	1.7992(18)
P(1)–C(13)	1.812(2)	P(1)–C(19)	1.8032(18)
P(1)–C(19)	1.815(2)	N(2)–C(6)	1.288(2)
N(2)–C(6)	1.274(3)	C(6)–C(5)	1.503(2)
C(6)–C(5)	1.500(3)	C(5)–N(1)	1.355(2)
C(5)–N(1)	1.358(3)	N(1)–C(1)	1.346(2)
N(1)–C(1)	1.341(3)		
Bond angles (°)			
C(25)–Rh(1)–P(1)	93.83(7)	N(1)–Pd(1)–P(1)	83.78(4)
N(1)–Rh(1)–P(1)	82.71(4)	P(1)–Pd(1)–Cl(2)	93.530(17)
C(25)–Rh(1)–Cl(1)	93.46(7)	N(1)–Pd(1)–Cl(1)	91.28(4)
N(1)–Rh–Cl(1)	90.21(4)	Cl(2)–Pd(1)–Cl(1)	92.021(16)
C(25)–Rh(1)–N(1)	175.40(8)	N(1)–Pd(1)–Cl(2)	173.10(4)
P(1)–Rh(1)–Cl(1)	171.768(19)	P(1)–Pd(1)–Cl(1)	172.287(17)
O(1)–C(25)–Rh(1)	179.2(2)	N(2)–P(1)–Pd(1)	104.60(5)
N(2)–P(1)–Rh(1)	105.40(6)	C(6)–N(2)–P(1)	120.39(13)
C(6)–N(2)–P(1)	122.30(14)	C(5)–C(6)–N(2)	124.00(16)
N(2)–C(6)–C(5)	123.96(18)	N(1)–C(5)–C(6)	119.77(15)
N(1)–C(5)–C(6)	118.76(17)	C(1)–N(1)–C(5)	118.62(15)
C(1)–N(1)–C(5)	117.84(17)		

Table 3
Selected bond lengths and angles for [$PtCl_2$(**1**-κ^2-P–N)] (**6**) and [PtCl(Me)(**1**-κ^2-P–N)] (**7**)

Complex **6**		Complex **7**	
Bond distances (Å)			
Pt(1)–N(1)	2.056(4)	Pt(1)–N(1)	2.174(3)
Pt(1)–P(1)	2.1898(12)	Pt(1)–P(1)	2.1643(9)
Pt(1)–Cl(1)	2.3601(12)	Pt(1)–Cl(1)	2.3613(9)
Pt(1)–Cl(2)	2.2817(12)	Pt(1)–C(25)	2.040(4)
P(1)–N(2)	1.684(4)	P(1)–N(2)	1.694(3)
P(1)–C(13)	1.805(5)	P(1)–C(13)	1.813(4)
P(1)–C(19)	1.798(5)	P(1)–C(19)	1.808(3)
N(2)–C(6)	1.285(6)	N(2)–C(6)	1.289(4)
C(6)–C(5)	1.489(6)	C(6)–C(5)	1.504(5)
C(5)–N(1)	1.353(6)	C(5)–N(1)	1.350(5)
N(1)–C(1)	1.343(6)	N(1)–C(1)	1.345(4)
Bond angles (°)			
N(1)–Pt(1)–P(1)	84.50(11)	N(1)–Pt(1)–P(1)	85.29(8)
P(1)–Pt(1)–Cl(2)	94.55(4)	P(1)–Pt(1)–C(25)	93.78(12)
N(1)–Pt(1)–Cl(1)	89.91(11)	N(1)–Pt(1)–Cl(1)	91.95(8)
Cl(2)–Pt(1)–Cl(1)	91.15(4)	C(25)–Pt(1)–Cl(1)	89.42(11)
N(1)–Pt(1)–Cl(2)	178.26(11)	N(1)–Pt(1)–C(25)	173.80(14)
P(1)–Pt(1)–Cl(1)	173.15(4)	P(1)–Pt(1)–Cl(1)	174.87(3)
N(2)–P(1)–Pt(1)	104.81(15)	N(2)–P(1)–Pt(1)	107.47(10)
C(6)–N(2)–P(1)	122.2(4)	C(6)–N(2)–P(1)	123.7(3)
C(5)–C(6)–N(2)	123.6(4)	C(5)–C(6)–N(2)	124.1(3)
N(1)–C(5)–C(6)	120.6(4)	N(1)–C(5)–C(6)	119.2(3)
C(1)–N(1)–C(5)	118.8(4)	C(1)–N(1)–C(5)	117.8(3)

generally an extremely poor indicator of P–N bond order. Consistent with the lack of P–N multiple bonding are the imine N(2)–C(6) and C(6)–C(5) bond distances, which are in accord with an imine and C–C single bond, respectively [6,31].

3. Reactivity of palladium(II) complexes of 1

3.1. Cationic palladium(II) methyl complexes of ligand 1

With a view to exploring the reactivity of the palladium methyl bond of complex **5** toward CO and ethene, it was of interest to prepare the corresponding cationic Pd systems. Thus, the palladium-methyl salts [PdMe(MeCN)(**1**-κ^2-P–N)][Z] **9** {Z = B{3,5-$(CF_3)_2$-C_6H_3}$_4$} and **10** {Z = PF_6} were prepared by reacting acetonitrile solutions of **5** with the sodium salts of the desired anion at RT for 4 and 3 days, respectively (Scheme 3). The two complexes were isolated as their acetonitrile adducts in good yields (91% and 81%, respectively). Selected NMR data for complexes **9** and **10** are presented in Table 1.

The $^{31}P\{^1H\}$ NMR spectrum of **9** exhibits a single, sharp resonance, whereas the spectrum of **10** features a broadened signal (vide infra). For both complexes only a very small change in ^{31}P NMR chemical shift (~0.5 ppm) is observed following chloride abstraction. In their $^{13}C\{^1H\}$ NMR spectra a significant shift of the resonance for the Pd–CH_3 group is observed, from δ −0.71 (**5**) to δ +0.71 and δ +1.24 for **9** and **10**, respectively. This is believed to result from the more electron deficient metal centre de-shielding the carbon of the methyl group. In both complexes, as with **5**, the Pd–CH_3 resonance appears as a singlet, indicating a Me *cis* to P geometry at palladium [32].

Sharp resonances corresponding to bound MeCN are observed in both the ^1H and $^{13}C\{^1H\}$ NMR spectra of **9**. In contrast, for the PF_6^- salt **10** no resonances could be observed for MeCN in either the ^1H or $^{13}C\{^1H\}$ NMR spectra ($CDCl_3$), while the resonance for the Pd–CH_3 group appeared slightly broadened in the ^1H NMR spectrum at ambient temperature. This is suggestive of reversible association/dissociation of MeCN at a rate comparable with the NMR timescale, possibly as a result of a competitive metal-binding interaction by the PF_6^- anion. No such process is observed for **9** since the $[B\{3,5\text{-}(CF_3)_2\text{-}C_6H_3\}_4]^-$ anion is known to be essentially non-coordinating, and hence does not compete with MeCN for binding to the metal centre [33].

In attempts to study the dynamic process associated with **10**, ^1H and $^{31}P\{^1H\}$ NMR spectra were obtained over the temperature range 300–230 K (10 K intervals; $CDCl_3$). No resonance attributable to MeCN (bound or free) was detectable according to ^1H NMR spectroscopy (even at 230 K), while the Pd–CH_3 resonance actually broadened slightly [$\nu_{1/2}$(300 K) = 4.2 Hz, $\nu_{1/2}$ (230 K) = 6.0 Hz]. However, examination of the $^{31}P\{^1H\}$ NMR spectra obtained on cooling the sample to 230 K, revealed that the broad resonance sharpened {$\nu_{1/2}$(300 K) = 14.3 Hz, $\nu_{1/2}$(230 K) = 3.5 Hz}, presumably due to a slowing in the rate of exchange of the MeCN. No variation was observed in the $^{31}P\{^1H\}$ NMR spectra for the resonance associated with the PF_6^- anion, which remained a septet over the temperature range 300–230 K.

3.2. Insertion reactions of neutral palladium(II) methyl complexes of ligand 1

The preparation of [PdCl{η^1-C(=O)Me}(**1**-κ^2-P–N)] (**12**), from a $CDCl_3$ solution of **5** under an atmosphere of CO at RT was carried out (Scheme 4). On following this reaction by $^{31}P\{^1H\}$ NMR spectroscopy, a single new species **12** {δ: +56.1} was observed to form, the initially yellow solution slowly turning bright red; complete conversion was achieved in 2 days. The identity of this new product **12** as the corresponding η^1-acyl derivative is clear from both ^1H {–C(O)*Me* δ: 2.04 ($^4J_{PH}$ = 1.7 Hz)} and $^{13}C\{^1H\}$ NMR spectroscopies {–*C*(O)Me

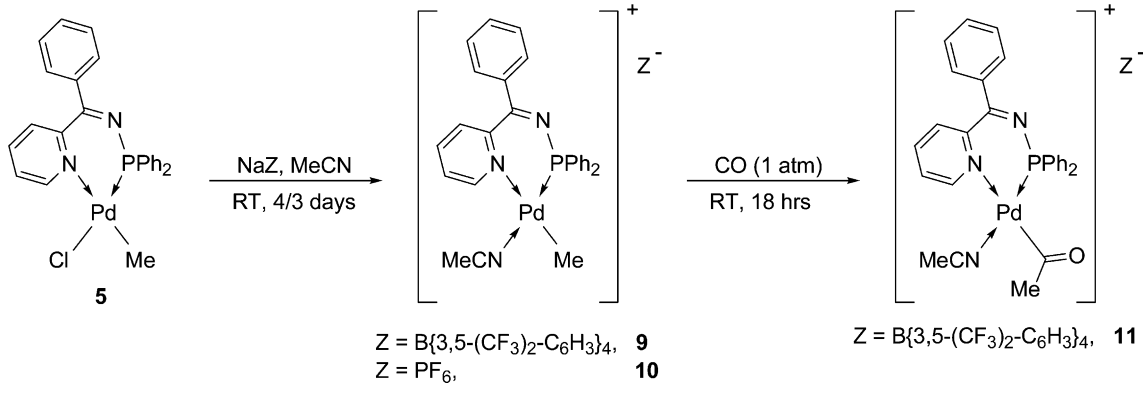

5

Z = B{3,5-$(CF_3)_2$-C_6H_3}$_4$, **9**
Z = PF_6, **10**

Z = B{3,5-$(CF_3)_2$-C_6H_3}$_4$, **11**

Scheme 3. Synthesis of cationic palladium(II) methyl complexes of ligand **1**.

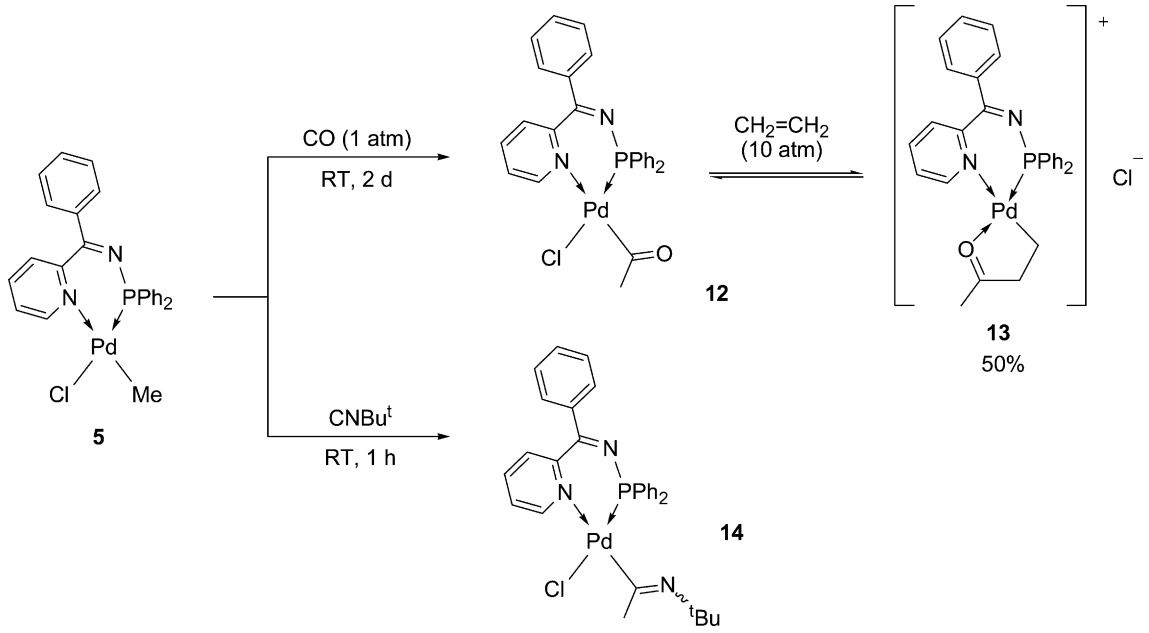

Scheme 4. Insertion reactions of neutral palladium complex **5**.

δ: 227.0 ($^2J_{PC}$ = 9 Hz)} and from IR spectroscopy, which reveals a characteristic carbonyl stretch at 1696 cm^{-1} [26,34–36]. The small magnitude of the value for $^2J_{PC}$ is indicative of a 'C *cis* to P' geometry at palladium, which is expected from *trans*-influence arguments [32]. The carbon of the methyl group of the acyl moiety appears as a doublet [δ: 39.0 ($^3J_{PC}$ = 25 Hz)] at a shift consistent with that observed for other acyl complexes [26,34].

A number of pathways for the formation of **12** from **5** are possible, all of which involve migratory insertion and isomerisation, but that differ in the nature of the initially formed CO complex: (a) via a 5-coordinate CO adduct; (b) through halide displacement followed by CO binding; and (c) following opening of the P–N chelate and subsequent CO coordination [35,37,38]. Since no intermediate species were observed by $^{31}P\{^1H\}$ NMR spectroscopy at room temperature (the necessary insertion reactions are known to be rapid [39]) and no detailed kinetic study was undertaken, no conclusion as to the mechanism for the formation of the acyl complex **12** may be made.

The insertion of ethene into the palladium–acyl bond of **12** represents another important step in the catalytic cycle of carbon monoxide/ethene copolymerisation [23,40]. To study this type of reaction with systems involving ligand **1**, a $CDCl_3$ solution of **12** was placed under an atmosphere of ethene and the reaction monitored by ^1H and $^{31}P\{^1H\}$ NMR spectroscopies. After 3 days no reaction had occurred. Consequently, the pressure of ethene was increased to ten atmospheres, which led to the rapid formation of a new species **13** in a near 1:1 ratio with the starting acyl complex **12**, by ^{31}P NMR spectroscopy. In the ^1H NMR spectrum (Fig. 5) the methyl group of **13** appears as a singlet (**d**), the β-CH_2 protons (**c**) as a pseudo-triplet of doublets, and the α-CH_2 protons (**b**) appear as a multiplet. It is proposed that the **13** forms via ethene insertion and halide displacement, resulting in an intramolecularly-coordinating ketone moiety [Pd{CH_2CH_2C-(=O)Me-κ^2-C–O}(**1**-κ^2-P–N)][Cl] (**13**) {^{31}P NMR δ: +72.9}.[2] This is in accord with considerable literature precedent in favour of the κ^2-C–O isomer over the non-chelating β-ketoalkyl form [13,21,41]. Although, no mechanistic detail may be inferred for this process without detailed kinetic studies, the reluctance for ethene insertion is likely to result from a combination of steric inhibition of initial substrate binding (considerably less facile for C_2H_4 compared with CO) and necessary isomerisation post insertion [18,41]. As expected on thermodynamic grounds, insertion of CO into the acyl bond of **13** could not be detected.

No further changes were observed by NMR spectroscopy over a period of 18 h at RT. Venting the over pressure of ethene led to the clean regeneration of **12** and the disappearance of **13**. Together, these observations suggest that an equilibrium situation has been achieved.

Although, both the insertion of ethene into palladium–acyl bonds [13,42,43] and the insertion of carbon monoxide into palladium–alkyl bonds [44] are known to be facile, the rates of these processes (and those of the corresponding de-insertion reactions) are known to differ significantly. This is reflected in this study by the

[2] Although IR spectroscopy would distinguish between the two possible isomers of **13**, high pressure facilities were not available to us.

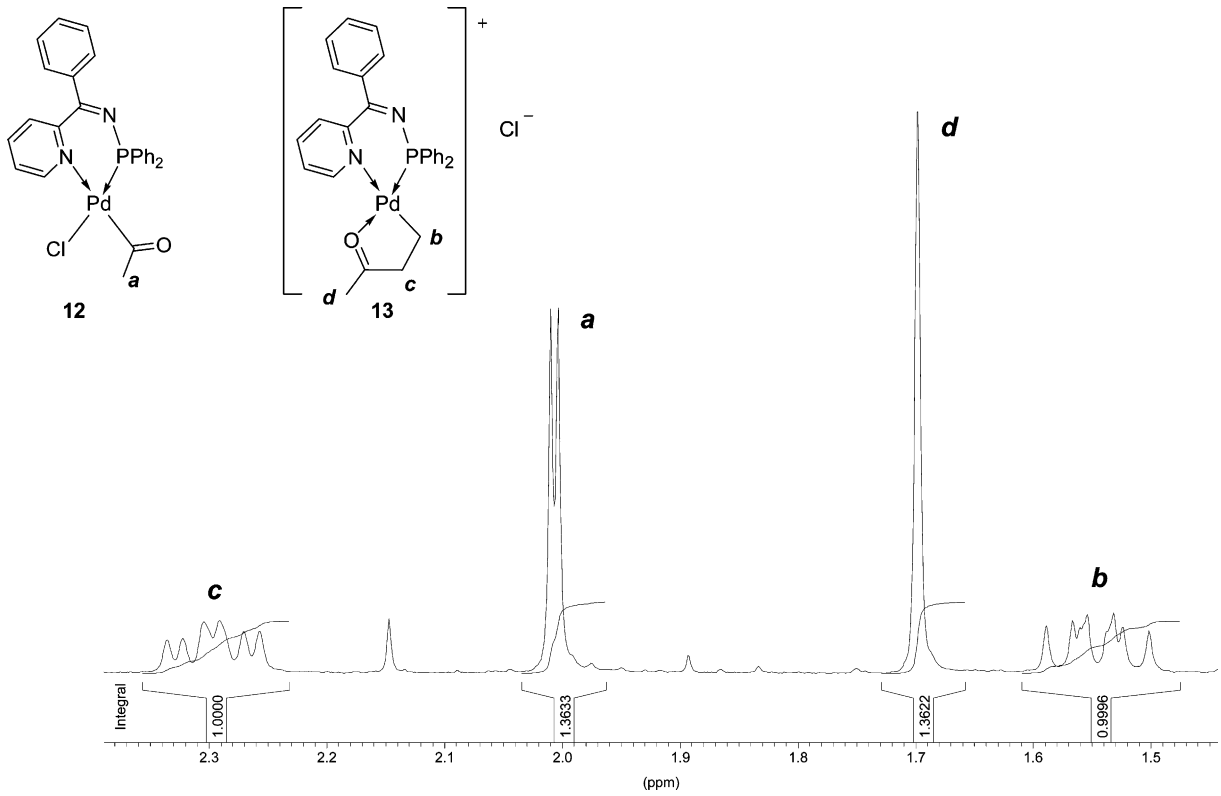

Fig. 5. ^{1}H (250.13 MHz, $CDCl_3$) NMR spectrum of the reaction of [PdCl{η^1-C(=O)Me}(**1**-κ^2-P–N)] (**12**) with C_2H_4 (10 atm) and proposed structure of **13**.

relative ease of formation of **12** from **5** (pCO = 1 atm) compared with that of **13** from **12** (pC_2H_4 = 10 atm). Indeed, studies of CO/C_2H_4 copolymerisation have identified that the rate of copolymerisation is dependent upon ethene pressure, with ethene insertion being the rate-determining step [23,45].

Capitalising on the successful formation of the acyl complex **12**, it was of interest to explore the related insertion of isonitriles (isoelectronic with CO). Thus, the iminoacyl complex [PdCl{η^1-C(=NBu^t)Me}(**1**-κ^2-P–N)] (**14**), was synthesised through addition of one equivalent of CNBu^t to a $CDCl_3$ solution of **5**; complete conversion to the product **14** occurred within 1 h at RT. This much higher rate of insertion of isonitrile compared with CO (conversion of **5** to **12**, 2 days) is in line with previous observations [46,47].

The $^{31}P\{^{1}H\}$ NMR spectrum of **14** shows a single sharp resonance at a chemical shift {δ: +57.9} almost identical to that for the acyl complex **12**. The arrangement about the palladium centre is proposed as being iminoacyl *cis* to P on *trans*-influence grounds, the moderate magnitude of two-bond coupling to the iminoacyl *C*=N being supportive of this assignment {δ: 148.9 ($^{2}J_{PC}$ = 24 Hz)} [32]. The methyl group of the iminoacyl moiety appears at characteristic shifts in the ^{1}H and $^{13}C\{^{1}H\}$ NMR spectra {^{1}H, δ: 2.85 ($^{4}J_{PH}$ = 2.1 Hz); ^{13}C, δ: 34.9 ($^{3}J_{PC}$ = 4 Hz)}. The $^{13}C\{^{1}H\}$ NMR shift of the *C*=N fragment is entirely consistent with an η^1-iminoacyl {δ: 148.92 ($^{2}J_{PC}$ = 23.5 Hz)} [36].

Complexes of η^1-iminoacyls normally show a strong C=N stretch in the region 1580–1630 cm^{-1} [36], with N-*tert*-butyl-substituted variants often appearing at the lower end of this scale [48]. However, since only a single C–N band was observed in the IR spectrum of **14** at 1593 cm^{-1} (cf. 1587 cm^{-1} for **1**), it seems reasonable to suggest that both the bands due to bound **1** and the C=N stretch of the η^1-iminoacyl are coincident.

Although CO double insertion is precluded on thermodynamic grounds, multiple isonitrile insertion is possible [47]. Here, addition of two equivalents of CNBu^t to **5** gave a number of new products according to ^{1}H and $^{31}P\{^{1}H\}$ NMR spectroscopies, which were not readily identifiable. However, complete consumption of **5** was clear, with no evidence for the formation of **14**. This is consistent with multiple CNBu^t insertion having indeed taken place.

3.3. Reactions of cationic palladium(II) methyl complexes of ligand *1*

A $CDCl_3$ solution of [PdMe(MeCN)(**1**-κ^2-P–N)][B{3,5-$(CF_3)_2$-C_6H_3}$_4$] (**9**) was placed under one atmosphere of CO. Complete conversion to the corresponding acyl derivative [Pd{C(=O)Me}(MeCN)(**1**-κ^2-P–N)][B{3,5-$(CF_3)_2$-C_6H_3}$_4$] (**11**) was achieved after 6 h

at RT (Scheme 3). Clearly, this reaction is considerably faster than that for the formation of the neutral acyl complex **12** from **5** (2 days, RT). This is consistent with the proposal that the rate-limiting step in these insertion reactions is believed to be initial binding of the substrate to the metal, something that will be facilitated for the coordinatively unsaturated cationic palladium systems.

The $^{31}P\{^{1}H\}$ NMR spectrum of **11** shows a single resonance (δ: +57.8) at a shift similar to that of the neutral η^1-acyl palladium species **12** (δ: +56.1). In the $^{13}C\{^{1}H\}$ NMR spectrum the carbonyl carbon of the acyl group appears as a downfield singlet with a chemical shift characteristic for an η^1-acyl complex (δ: 222.8), the multiplicity indicating that the acyl lies *cis* to phosphorus [32]. As with the precursor complex **9**, MeCN is tightly bound to palladium, sharp resonances appearing in the ^{1}H and $^{13}C\{^{1}H\}$ NMR spectra for this ligand {^{1}H, δ: 2.15; ^{13}C, δ: +2.50}. The methyl group of the acyl moiety gives rise to a resonance at δ: 38.0 ppm, consistent with that observed for **12** and other η^1-acyl complexes. FAB mass spectrometry supports the assignment of **11** as the acetonitrile adduct, clearly showing loss of both the acyl and MeCN ligands [*m/z*: 515 $(M–CH_3CN)^+$, 472 $(M–CH_3CN\text{-acyl})^+$].

The IR spectrum of **11** shows an acyl CO band at 1653 cm^{-1}. This is at a significantly lower frequency to that observed for **12** (1696 cm^{-1}) and is likely to result from some slight interaction between the acyl oxygen and the cationic metal centre, although this is insufficient to displace MeCN. It is well recognised that true η^2-acyl complexes show ν_{CO} bands at lower frequencies than their η^1-acyl counterparts (usually $\Delta\nu_{CO} > 50$ cm^{-1}) [36].

In contrast, attempts to bind and subsequently insert ethene into the Pd–Me bond of **11** proved elusive. Under 1 atmosphere of ethene no reaction was observed to occur by either ^{1}H or ^{31}P NMR spectroscopy (as for the neutral system). In contrast, at elevated temperatures or pressures, rapid decomposition of **11** occurred, with the generation of palladium 'black' and other intractable products.

3.4. Catalytic CO/ethene copolymerisation testing

Although homoditopic N–N [49–52] and P–P [23,53–55] ligand systems have received the most attention for CO/ethene copolymerisation, there is a growing body of evidence that heteroditopic P–N ligands are also effective [21,56–58]. For polyketone synthesis, a bite angle dependency has been noted for both P–P- and P–N-based scaffolds, 6-membered chelate systems being preferential in terms of activity, selectivity, and polymer molecular weight [23,58–60]. Thus, the combination of the size of chelate formed and the reactivity demonstrated (vide supra) by ligand **1** in partnership with palladium toward CO and ethene, made this an intriguing system to explore for this type of polymerisation reaction.

The behaviour of both preformed complex [$PdCl_2$(**1**-κ^2-P–N)] (**4**) (entries 1–3, Table 4) and systems generated in situ from $Pd(OAc)_2$ and ligand **1**, in a 1:1.5 ratio (entries 4–6), were explored at both 30 and 90 °C under 38 bar pressure of pre-mixed 1:1 CO:C_2H_4. All tests were performed in dry methanol with 4 equivalents of methanesulphonic acid as an activator, conditions representative of those generally used for the formation of polyketones [23].

Contrary to expectations, none of the reactions (entries 1–6) led to the formation of polyketone. Indeed, no new carbon-containing species could be detected from reactions performed at 30 °C (entries 1 and 4). In contrast, for tests carried out at 90 °C in the presence of the acid activator (entries 2 and 5), 4-oxo-hexanoic acid methyl ester (**15**) was obtained as the only organic product, with an activity of ca. 8–9 g $\{mol\ Pd\}^{-1}\ bar^{-1}\ h^{-1}$ (Scheme 5). Although these values are only moderate, they are of a comparable magnitude to the activities for the formation of CO/C_2H_4 copolymers by other P–N ligand-based catalyst systems: 9 g $(mol\ Pd)^{-1}\ bar^{-1}\ h^{-1}$ by Green et al. [56]; 148 g $(mol\ Pd)^{-1}\ bar^{-1}\ h^{-1}$ by Fryzuk et al. [57]; and 224 g $(mol\ Pd)^{-1}\ bar^{-1}\ h^{-1}$ by Liu et al. [58].

Notably, analysis of the organic phase isolated after each catalytic test revealed that no methyl propionate

Table 4
Summary of ethene/carbon monoxide oligomerisation chemistry catalysed by preformed complex **4** or by an initiator generated in situ from $[Pd(OAc)_2]$ and **1**[a]

Entry	Initiator	[Pd] (Mol × 10^{-4})	Activator[c]	Temperature (°C)	Oligomer yield (g)	Activity for oligomers[d]
1	**4**	1.80	$MeSO_3H$	30	0	0
2	**4**	1.80	$MeSO_3H$	90	0.166	8.0
3	**4**	1.80	None	90	0	0
4	$Pd(OAc)_2$/**1**[b]	1.82	$MeSO_3H$	30	0	0
5	$Pd(OAc)_2$/**1**[b]	1.82	$MeSO_3H$	90	0.180	8.7
6	$Pd(OAc)_2$/**1**[b]	1.82	None	90	0	0

[a] Reaction conditions: MeOH (60 mL) solvent, stirring rate (900 rpm), 1:1 ethene:carbon monoxide (38 bar), 3 h.
[b] Ratio $[Pd(OAc)_2]$:**1** = 1:1.5.
[c] Pd:$MeSO_3H$ = 1:4.
[d] g $(mol\ Pd)^{-1}\ bar^{-1}\ h^{-1}$.

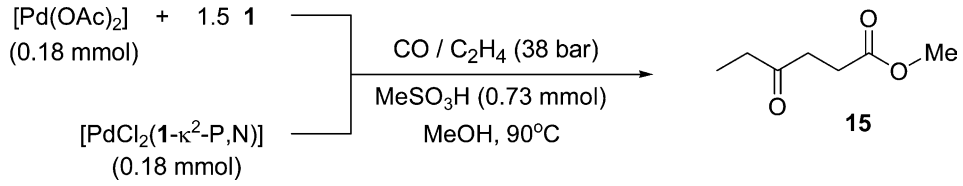

Scheme 5. Formation of 4-oxo-hexanoic acid methyl ester (**15**) from CO/C_2H_4/MeOH.

had been formed via mono-hydromethoxycarbonylation. This side product is often observed to form with poorly active polyketone initiators [23]. Irrespective of the reaction conditions, a large amount of colloidal 'palladium black' was found at the end of each run.

The nature of the catalytically active species generated in situ (entries 4–6) was probed through investigation of the reaction between $Pd(OAc)_2$ and **1** (1:1) in MeOH. After 30 min at room temperature, a vivid red-orange solution had been formed, which was found to contain five new species all with chemical shifts characteristic of metal-bound aminophosphines (Δ: +58 to +82 ppm), in addition to a small quantity of unbound **1**, according to $^{31}P\{^1H\}$ NMR spectroscopy. Although this mixture remained unchanged over a period of 18 h at RT, its complexity precluded further analysis. Subsequent heating of the solution at reflux for a further 18 h led to the formation of 'palladium black' and a green solution, which showed no signal by $^{31}P\{^1H\}$ NMR spectroscopy. Although not revealing the identity of the active catalytic species, these observations confirm both the partial resilience of unbound **1** and its complexes in MeOH, despite the presence of a potentially reactive polar P–N linkage, in line with previous observations regarding the stability of metal-bound aminophosphines [7,8].

$$Pd^{2+} + MeOH \rightarrow [Pd\text{-}OMe]^+ + H^+ \quad (1)$$

$$[Pd\text{-}OMe]^+ \rightarrow [Pd\text{-}H]^+ + HC(O)H \quad (2)$$

It is believed that keto-ester **15** results from either a catalytic cycle based upon an initial Pd-hydride or Pd–OMe species (Scheme 6), generated in situ from the MeOH solvent (equations 1 and 2); such mechanisms are well established for polyketone synthesis [23,45,61]. Chain termination by methanol can occur via protonation of the β-ketoalkyl (cycle **A**) or by nucleophilic attack at the acyl complex (cycle **B**), however the structure of **15** cannot be used to distinguish these two processes. As would be expected from the proposed mechanisms for the formation of **15**, no organic products are obtained when anhydrous dichloromethane is used in the place of MeOH as solvent. Although there is no evidence here in preference of either pathway **A** or **B**, methyl propionate formation is generally believed to result from a palladium hydride-based cycle [62]. However, the unique selectivity for the formation of keto-ester **15** via palladium-catalysed copolymerisation of CO/C_2H_4 with ligand **1** merits further comment, since a Schulz–Flory distribution of oligomeric products would normally be expected [2,3].

For palladium-based initiators bearing chelating P–P and N–N donors it is well documented that the nature of the ligand (bite angle {bridge length}, steric bulk, bridge substituents and basicity) has a considerable impact upon the polymerisation process (especially activity and product distribution) [2,3,45,63,64]. Not only is it reasonable to suggest that these types of effect are also likely to play an important role for heteroditopic ligands, but that the electronic asymmetry (differences in *trans* effect) in the chelate will also be significant [18,65]. Although the formation of polyketone is often favoured over lower molecular weight oxygenates for P–P-based ligands that adopt 6-membered chelates [23], there are notable exceptions [2,61,66].

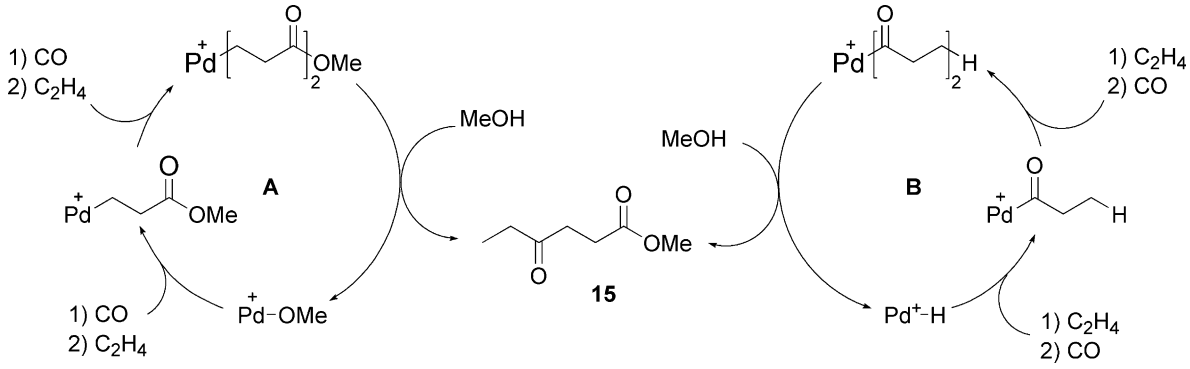

Scheme 6. 'Carbomethoxy' (**A**) and 'hydride' (**B**) catalytic cycles for the formation of keto-ester (**15**) from CO/C_2H_4/MeOH.

Ligand **1** is somewhat flexible and can readily accommodate P–N bite angles of 90° or 120°. This feature is important since **1** can bind to both square planar and trigonal bipyramidal complexes, something that is known to influence not only migratory insertion pathways, but also dictate between oligomerisation and polymerisation [67]. The 'distorted boat' conformation that **1** adopts provides a degree of steric hindrance above and below the square coordination plane of palladium, which could slow insertion reactions. Consideration of the molecular structure of **4** (Fig. 2) indicates that the orientation of P(1) locates one of its phenyl substituents in reasonable proximity to Cl(2). In solution, rotation about the P(1)–C(13) bond would further enhance this effect. As has been demonstrated, the aminophosphine component of **1** is a somewhat poor σ-donor, something that will enhance the nucleophilicity of the palladium to which it is bound. Under the catalytic conditions employed, this will favour attack of methanol at the acyl generated during the 'hydride cycle' **B**, leading to more rapid chain termination and hence lower molecular weight products.

An informative comparison may be drawn with a related P–N ligand based on an aza-*N*-indolyl skeleton, reported recently by Burrows and co-workers [21]. Like **1**, this system combines an aromatic N- and an N-bound PPh_2-donor fragment, but differs in the constitution of the ligand backbone and in the formation of 5- rather a 6-membered metallacycle, with a slightly more electron-donating phosphine moiety. In contrast to **1**, when bound to palladium, Burrows' ligand leads exclusively to polyketone. The observed 'reversed' selectivity obtained with **1** compared to that of Burrows' system is believed to result from a the greater flexibility of the former (rotation being possible about the C(5)–C(6) and the P(1)–N(2) bonds), compared with planar aromatic azaindole backbone.

3.5. Conclusion

A versatile 'one-pot' synthesis of a 6-membered chelating P–N ligand **1** has been described via addition of phenyl lithium to 2-cyanopyridine and subsequent quenching with chlorodiphenyl phosphine. This ligand readily coordinates to rhodium(I), palladium(II) and platinum(II) in a predictable manner, as indicated both spectroscopically in solution and by X-ray crystallography in the solid state. The neutral palladium methyl complex **5** readily inserts CO and ^{t}BuNC to yield the corresponding η^1-acyl (**12**) and -iminoacyl (**14**) complexes, respectively. Under an elevated pressure of ethene, an equilibrium is established between **12** and the product resulting from insertion, **13**. Similar, but more rapid CO insertion chemistry has been established for the cationic methyl palladium(II) complex **9**, which affords an essentially η^1-acyl complex **11**, that demonstrates a weak secondary Pd–carbonyl interaction. The robustness of the inherent P–N linkage of **1** has been established.

A highly selective, but moderately active hydrocarboxylation catalyst system is obtained on combining ligand **1** with palladium(II) in the presence of methanesulphonic acid. 4-Oxo-hexanoic acid methyl ester (**15**) is obtained as the only organic product from the reaction of CO with C_2H_4 (38 bar, 90 °C) in methanol. The unusual selectivity of palladium(II) complexes of **1** for the formation of **15** is attributed to a combination of a significant steric demands, low basicity, and flexible P–N bite angle of this ligand framework.

Further variants of **1** have been prepared and optimisation of the hydrocarboxylation behaviour of palladium complexes of these types of ligand is being actively investigated.

4. Experimental

4.1. General considerations

All manipulations of air and/or water sensitive materials were performed under an atmosphere of nitrogen using standard Schlenk and cannula techniques or in a conventional nitrogen-filled glove box (unless stated otherwise). Solvents were freshly distilled under nitrogen from sodium/benzophenone (tetrahydrofuran, diethyl ether, toluene, dme), from calcium hydride (dichloromethane), from sodium (hexane, pentane, 40–60 PE), from magnesium/iodine (MeOH), or from P_2O_5 (CD_2Cl_2, C_6D_6 and $CDCl_3$) and degassed prior to use. Elemental analyses were performed by S. Boyer at London Metropolitan University. NMR were recorded on a Bruker AM 250, AMX 300, or AMX 400; chemical shifts were referenced to residual protio impurities in the deuterated solvent (^{1}H), to the deuterated solvent (^{13}C), or to external aqueous 85% H_3PO_4 (^{31}P). Chemical shifts are reported in ppm and coupling constants in Hz. All spectra were obtained at ambient probe temperature (298 K) unless stated otherwise. For ^{1}H NMR spectra, ^{31}P coupled resonances were verified by obtaining ^{1}H $\{^{31}P\}$ spectra. ^{13}C NMR spectra were assigned with the aid of DEPT 135. Infrared spectra were recorded (Nujol mulls [KBr windows], KBr discs, or in solution [KBr windows]) on a Perkin–Elmer 1600 spectrophotometer; Nujol was dried over sodium wire. FAB (3-nitrobenzyl alcohol matrix) and EI mass spectra were recorded on a Kratos Concept 1H instrument and are reported in (*m*/*z*). GC–MS were performed using a Perkin–Elmer Autosystem XL GC machine (PE-5MS 30 m coil, internal diameter = 0.25 mm, film thickness = 0.25 μm) coupled to a Perkin–Elmer Turbomass mass spectrometer. Sonication was achieved by suspending the desired

reaction vessel in a water-filled Grant Ultrasonic Bath XB2.

Palladium, platinum and rhodium salts were used on loan from Johnson Matthey. BAr^F_3 was a gift from the Asahi Glass Corporation. Gaseous reagents were from BOC and all other chemicals from Aldrich. All solid reagents were used as received, except 2-CN-pyridine which was distilled from CaH_2 under reduced pressure. Where appropriate, liquid reagents were dried, distilled and deoxygenated prior to use. Gases were passed through a drying column (silica/$CaCO_3$/P_2O_5) prior to use. *cis*-[$Mo(CO)_4(pip)_2$] [68], [$RhCl(CO)_2]_2$ [69], [$PdCl_2(MeCN)_2$] [70], [PdCl(Me)(COD)] [71], [$PdMe_2$(TMEDA)] [72], [$PtCl_2$(COD)] [73], [PtCl(Me)(COD)] [74], [$PtMe_2$(COD)] [75], and [$NaB(3,5\text{-}(CF_3)_2C_6H_4)_4$] [76] were prepared according to literature procedures. All other chemicals were obtained commercially and used as received. Melting points were obtained in sealed glass tubes under nitrogen, using a Gallenkamp Melting Point apparatus and are uncorrected.

4.2. Diphenylphosphino(phenyl pyridin-2-yl-methylene)amine (*1*)

To a stirred, cooled (−78 °C) solution of dried 2-cyano-pyridine (4.00 g, 3.84×10^{-2} mol) in diethyl ether (300 mL) was added dropwise PhLi (1.8 M, cyclohexane/diethyl ether, 21.4 mL, 3.84×10^{-2} mol), and the vessel left to stir at this temperature for 4 h, yielding a dark red solution. An ethereal solution (50 mL) of Ph_2PCl (6.9 mL, 3.84×10^{-2} mol) was added dropwise via cannula. The mixture was allowed to stir at −78 °C for 1 h before being left to warm to RT with stirring for 18 h, resulting in a brown solution and white precipitate. The solid was removed by filtration through a glass frit and washed with diethyl ether (2 × 50 mL) to leave a transparent brown solution. The solvent was removed in vacuo to leave a brown solid, which was subsequently extracted with hexane (300 mL) using a Soxhlet apparatus. Upon cooling, the resultant red solution precipitated **1** (Fig. 6) as a powdery yellow-orange solid, which was recovered by cannula filtration (6.29 g, 45%, m.p. = 99–101 °C). ^{1}H NMR (250.13 MHz, C_6D_6): δ [ppm] = 8.52 (1 H, m, C^1*H*), 7.93–7.85 (5H, m, Py*H* + C_6H_5), 7.66 (1H, dt, $^3J_{HH}$ = 7.8, $^3J_{HH}$ = 1.2, C*H*), 7.34–7.14 (11H, m, Py*H* + C_6H_5), 6.75 (1H, dd, $^3J_{HH}$ = 4.8, $^3J_{HH}$ = 1.1, C*H*). ^{13}C {^{1}H} NMR (100.61 MHz, $CDCl_3$): δ [ppm] = 171.8 (d, $^2J_{PC}$ = 7, *C*^{6}), 156.9 (d, $^3J_{PC}$ = 6, *C*^{5}), 149.3 (s, *C*^{1}), 141.9 (d, $^3J_{PC}$ = 11, *C*^{7}), 139.6 (d, $^1J_{PC}$ = 6, {*i*-C_6H_5}$_2$P), 136.1 (s, *C*^{3}), 132.1 (d, $^2J_{PC}$ = 21, {*o*-C_6H_5}$_2$P), 130.2 (s, *C*^{10}), 128.7 (d,$^4J_{PC}$ = 3, {*p*-C_6H_5}$_2$P), 128.6 (s, *C*^{8}), 128.3 (s, *C*^{9}), 128.3 (d, $^3J_{PC}$ = 2, {*m*-C_6H_5}$_2$P), 123.8 (s, *C*^{2}), 123.5 (d, $^4J_{PC}$ = 2, *C*^{4}). ^{31}P {^{1}H} NMR (101.26 MHz, C_6D_6): δ [ppm] = +37.6 (s); (101.26 MHz, CD_2Cl_2) δ: +41.9 (s). MS (FAB$^+$): 366 M$^+$, 289 (M–Ph)$^+$. IR (KBr, $CDCl_3$ solution): ν(C=N) = 1584 cm^{-1}. *Anal.* Found C, 78.78; H, 5.35; N, 7.52%. Calc. for $C_{24}H_{19}N_2P$ (366.39): C, 78.67; H, 5.23; N, 7.65%.

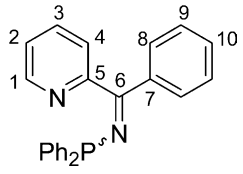

Fig. 6. General numbering scheme for **1** for NMR assignment.

4.3. Diphenylphosphino selenide (phenyl pyridin-2-yl-methylene) amine (*2*)

A Young's tap NMR tube was charged with Se (19 mg, 2.36×10^{-4} mol) and **1** (72 mg, 1.97×10^{-4} mol) and the tube sealed, before transferring to a Schlenk line. $CDCl_3$ (0.75 mL) was added and the tube freeze/thaw degassed, back-filled with N_2 and sealed. The tube was then sonicated for 18 h. The yellow solution turned green. Excess Se was removed via filtration, to leave a transparent dark green solution of **2**. ^{31}P {^{1}H} NMR (101.26 MHz, $CDCl_3$): δ [ppm] = +42.6 (s with satellites, $^1J_{SeP}$ = 769).

4.4. Diphenylphosphino(phenyl pyridin-2-yl-methylene)amine rhodium carbonyl chloride, [RhCl(CO)(*1*-κ^2-*P*–*N*)] (*3*)

A Young's tap NMR tube was charged with **1** (51 mg, 1.39×10^{-4} mol), [$Rh(CO)_2Cl]_2$ (27 mg, 6.95×10^{-5} mol) and sealed, before transferring to a Schlenk line. $CDCl_3$ (0.75 mL) was added and the tube freeze/thaw degassed, back-filled with N_2 and sealed. After 30 min, when gas evolution had finished, the solution was freeze/thaw degassed, back-filled with an atmosphere of CO, sealed and left to stand at RT for 1 h, resulting in a deep red solution. Layering petroleum ether 40–60 on top of the $CDCl_3$ solution, yielded crystals of **3** suitable for an X-ray structure determination, after standing for 1 week. A CO atmosphere was found to be necessary to prevent decomposition of **3** in solution, as has been reported previously[3] [22]. ^{1}H NMR (301.24 MHz, $CDCl_3$): δ [ppm] = 9.60 (1H, d, $^3J_{HH}$ = 5.2, C^1*H*), 7.69–7.19 (17H, m, Py*H* + C_6H_5), 7.13 (1H, d, $^3J_{HH}$ = 7.9, C*H*). ^{13}C {^{1}H} NMR (75.75 MHz, CD_2Cl_2): δ [ppm] = 188.1 (br, $\nu_{1/2}$ = 48 Hz, Rh–*C*O), 176.5 (s, *C*^{6}), 154.7 (s, *C*^{1}), 147.7 (d, $^3J_{PC}$ = 20, *C*^{5}), 139.0 (s, *C*^{3}), 138.7 (d, $^3J_{PC}$ = 16, *C*^{7}),

[3] Complex **3** is stable in solution under an atmosphere of CO for weeks.

135.4 (dd, $^1J_{PC}$ = 61, $^2J_{RhC}$ = 2.0, {*i*-C_6H_5}$_2$P), 132.6 (s, C^{10}), 132.0 (d, $^2J_{PC}$ = 13, {*o*-C_6H_5}$_2$P), 131.1 (d, $^4J_{PC}$ = 3, {*p*-C_6H_5}$_2$P), 129.9 (s, C^8), 128.7 (s, C^9), 128.5 (d, $^3J_{PC}$ = 11, {*m*-C_6H_5}$_2$P), 127.4 (s, C^2), 126.8 (s, C^4). ^{31}P {^{1}H} NMR (121.94 MHz, $CDCl_3$): δ [ppm] = +84.5 (d, $^1J_{RhP}$ = 167). MS (FAB^+): 497 ($M–Cl)^+$, 469 ($M–Cl–CO)^+$. IR (KBr, $CDCl_3$ solution): ν(CO) = 2010 cm^{-1}; ν(C=N) = 1608, 1589 cm^{-1}. *Anal.* Found C, 56.30; H, 3.55; N, 5.21%. Calc. for $C_{25}H_{19}N_2OPClRh$ (532.76): C, 56.36; H, 3.59; N, 5.26%.

4.5. Diphenylphosphino(phenyl pyridin-2-yl methylene)-amine palladium dichloride, [$PdCl_2$(**1**-κ^2-P–N)] (**4**)

A Schlenk was charged with **1** (365 mg, 9.97×10^{-4} mol) and $PdCl_2$(COD) (271 mg, 9.49×10^{-4} mol). The vessel was stirred and cooled (−78 °C), as CH_2Cl_2 (40 mL) was added dropwise, then left to stir and warm to RT over 18 h. The CH_2Cl_2 was removed under reduced pressure to leave **4** as a yellow powder, which was washed with diethyl ether (3 × 30 mL) and dried in vacuo (484 mg, 94%). Yellow needle-like crystals of **4**, suitable for an X-ray structure determination, were grown from a CD_2Cl_2 solution layered with hexane. ^{1}H NMR (250.13 MHz, CD_2Cl_2): δ [ppm] = 9.94 (1H, dd, $^3J_{HH}$ = 5.8, $^4J_{PH}$ = 1.2, C^1*H*), 7.81–7.27 (18H, m, Py*H* + C_6H_5). ^{13}C {^{1}H} NMR (75.75 MHz, CD_2Cl_2): δ [ppm] = 181.6 (d, $^2J_{PC}$ = 5, C^6), 157.4 (s, C^1), 145.3 (d, $^3J_{PC}$ = 21, C^5), 140.4 (s, C^3), 138.1 (d, $^3J_{PC}$ = 19, C^7), 134.2 (s, C^{10}), 133.3 (d, $^2J_{PC}$ = 11, {*o*-C_6H_5}$_2$P), 132.7 (d, $^4J_{PC}$ = 3, {*p*-C_6H_5}$_2$P), 130.9 (s, C^8), 129.9 (d, $^1J_{PC}$ = 70, {*i*-C_6H_5}$_2$P), 129.6 (s, C^9), 129.4 (s, C^2), 129.1 (d, $^3J_{PC}$ = 12.0, {*m*-C_6H_5}$_2$P), 128.6 (s, C^4). ^{31}P {^{1}H} NMR (101.26 MHz, CD_2Cl_2): δ [ppm] = +66.8 (s). MS (FAB^+): 544 M^+, 509 ($M–Cl)^+$, 472 ($M–2Cl)^+$. IR (KBr, $CDCl_3$ solution): ν(C=N) = 1608, 1587, 1560 cm^{-1}. *Anal.* Found C, 53.13; H, 3.43; N, 4.98%. Calc. for $C_{24}H_{19}N_2PCl_2Pd$(543.72): C, 53.02; H, 3.52; N, 5.15%.

4.6. Diphenylphosphino(phenyl pyridin-2-yl methylene)-amine palladium methyl chloride, [PdCl(Me)-(**1**-κ^2-P–N)] (**5**)

A Schlenk was charged with **1** (457 mg, 1.25×10^{-3} mol) and PdCl(Me)(COD) (321 mg, 1.21×10^{-3} mol). The vessel was cooled to −78 °C and the solids stirred, as CH_2Cl_2 (20 mL) was added dropwise. Subsequently, the vessel was kept at a constant 15 °C (cold water bath) and stirred for 2 days, with all light excluded. The resulting mixture was filtered to remove colloidal palladium, giving a transparent yellow solution. The CH_2Cl_2 was removed under reduced pressure to leave **5** as an orange-yellow powder, which was washed with hexane (3 × 30 mL) and dried in vacuo to leave a vivid yellow powder (551 mg, 87%). ^{1}H NMR (301.24 MHz, $CDCl_3$): δ [ppm] = 9.76 (1H, dd, $^3J_{HH}$ = 5.4, $^4J_{PH}$ = 1.0, C^1*H*), 7.67–7.20 (17H, m, Py*H* + C_6H_5), 7.08 (1H, d, $^3J_{HH}$ = 7.6, C*H*), 0.54 (3H, d, $^3J_{PH}$ = 3.2, Pd–CH_3). ^{13}C {^{1}H} NMR (75.75 MHz, $CDCl_3$): δ [ppm] = 177.3 (d, $^2J_{PC}$ = 4, C^6), 153.6 (s, C^1), 148.1 (d, $^3J_{PC}$ = 16, C^5), 139.2 (d, $^3J_{PC}$ = 16, C^7), 138.2 (s, C^3), 132.7 (d, $^1J_{PC}$ = 60, {*i*-C_6H_5}$_2$P), 132.7 (d, $^2J_{PC}$ = 13, {*o*-C_6H_5}$_2$P), 132.5 (s, C^{10}), 131.2 (d, $^4J_{PC}$ = 2, {*p*-C_6H_5}$_2$P), 130.0 (s, C^8), 128.6 (d, $^3J_{PC}$ = 4, {*m*-C_6H_5}$_2$P), 128.4 (s, C^9), 127.5 (s, C^2), 127.0 (s, C^4), −0.7 (s, Pd–CH$_3$). ^{31}P {^{1}H} NMR (121.94 MHz, $CDCl_3$): δ [ppm] = +72.9 (s). MS (FAB^+): 507 ($M–Me)^+$, 487 ($M–Cl)^+$, 472 ($M–Me–Cl)^+$. IR (KBr, $CDCl_3$ solution): ν(C=N) = 1608, 1589, 1564 cm^{-1}. *Anal.* Found C, 57.26; H, 4.15; N, 5.20%. Calc. for $C_{25}H_{22}N_2PClPd$ (523.30): C, 57.38; H, 4.24; N, 5.35%.

4.7. Diphenylphosphino(phenyl pyridin-2-yl methylene)-amine platinum dichloride, [$PtCl_2$(**1**-κ^2-P–N)] (**6**)

A Schlenk was charged with **1** (145 mg, 3.96×10^{-4} mol) and $PtCl_2$(COD) (144 mg, 3.85×10^{-4} mol). The solids were stirred, as CH_2Cl_2 (10 mL) was added dropwise. The vessel was sealed and left to stir for 4 days at RT, the initially orange solution turned yellow. The solution was filtered and the solvent removed under reduced pressure to leave **6** as a vivid yellow powder, which was washed with diethyl ether (3 × 10 mL) and dried in vacuo (219 mg, 90%). Yellow needle-like crystals of **6**, suitable for an X-ray structure determination, were grown from a CH_2Cl_2 solution layered with hexane. ^{1}H NMR (301.24 MHz, CD_2Cl_2): δ [ppm] = 10.10 (1H, dd, $^3J_{HH}$ = 5.9, $^4J_{PH}$ = 1.3, C^1*H*), 7.99 (1H, m, C*H*), 7.79–7.35 (18H, m, Py*H* + C_6H_5). ^{13}C {^{1}H} NMR (75.75 MHz, CD_2Cl_2): δ [ppm] = 180.7 (d, $^2J_{PC}$ = 5, C^6), 156.7 (s, C^1), 144.3 (d, $^3J_{PC}$ = 19, C^5), 140.1 (s, C^3), 138.3 (d, $^3J_{PC}$ = 19, C^7), 133.7 (s, C^{10}), 133.2 (d, $^2J_{PC}$ = 11, {*o*-C_6H_5}$_2$P), 132.5 (d, $^4J_{PC}$ = 2, {*p*-C_6H_5}$_2$P), 130.5 (s, C^8), 129.2 (s, C^9), 129.1 (d, $^1J_{PC}$ = 76, {*i*-C_6H_5}$_2$P), 129.0 (s, C^2), 128.8 (d, $^3J_{PC}$ = 12.0, {*m*-C_6H_5}$_2$P), 127.7 (s, C^4). ^{31}P {^{1}H} NMR (121.94 MHz, CD_2Cl_2): δ [ppm] = +39.5 (s + satellites, $^1J_{PtP}$ = 3806). MS (FAB^+): 597 ($M–Cl)^+$, 561 ($M–2Cl)^+$. IR (KBr, $CDCl_3$ solution): ν(C=N) = 1608, 1590, 1560 cm^{-1}. *Anal.* Found C, 45.67; H, 3.08; N, 4.58%. Calc. for $C_{24}H_{19}N_2PCl_2Pt$ (632.38): C, 45.58; H, 3.03; N, 4.43%.

4.8. Diphenylphosphino(phenyl pyridin-2-yl methylene)-amine platinum methyl chloride, [PtCl(Me)(**1**-κ^2-P–N)] (**7**)

A Young's tap NMR tube was charged with **1** (37 mg, 1.01×10^{-4} mol) and PtCl(Me)(COD) (36 mg, 1.01×10^{-4} mol). $CDCl_3$ (0.75 mL) was added and the tube freeze/thaw degassed, back-filled with N_2, sealed

and left to stand at RT for 18 h. The solvent was removed under reduced pressure to leave **7** as a yellow powder, which was washed with hexane (3×5 mL) and dried in vacuo (56 mg, 90%). Yellow crystals of **7** suitable for an X-ray structure determination were grown from CH_2Cl_2/petroleum ether 40–60. ^{1}H NMR (250.13 MHz, $CDCl_3$) δ: 9.94 (1H, dd + satellites, $^3J_{HH} = 5.5$, $^4J_{PH} = 0.9$, $^3J_{PtH} = 15.4$, C^1*H*), 7.76–7.17 (18H, m, Py*H* + C_6H_5), 0.53 (3H, d + satellites, $^3J_{PH} = 3.7$, $^2J_{PtH} = 79.9$, Pt–C*H*$_3$). ^{13}C {^{1}H} NMR (75.75 MHz, $CDCl_3$) δ: 177.4 (d, $^2J_{PC} = 5$, *C*^{6}), 153.6 (s, *C*^{1}), 145.7 (d, $^3J_{PC} = 15$, *C*^{5}), 139.3 (d, $^3J_{PC} = 17$, *C*^{7}), 137.9 (s, *C*^{3}), 132.8 (d + satellites, $^2J_{PC} = 12$, $^3J_{PtC} = 41$, {*i*-C_6H_5}$_2$P), 132.4 (s, *C*^{10}), 131.3 (d, $^1J_{PC} = 74$, {*i*-C_6H_5}$_2$P), 131.3 (d, $^4J_{PC} = 3$, {*p*-C_6H_5}$_2$P), 130.0 (s, *C*^{8}), 128.6 (s, *C*^{9}), 128.3 (d, $^3J_{PC} = 11$, {*m*-C_6H_5}$_2$P + *C*^{2} obscured here), 127.8 (s, *C*^{4}), −16.7 (d + satellites, $^2J_{PC} = 5$, $^1J_{PtC} = 677$, Pt–*C*H$_3$). ^{31}P {^{1}H} NMR (101.26 MHz, $CDCl_3$) δ: +46.9 (s + satellites, $^1J_{PtP} = 4800$). MS (FAB$^+$): 597 (M–Me)$^+$, 576 (M–Cl)$^+$. IR (KBr, $CDCl_3$ solution): ν(C=N) = 1610, 1590 cm^{-1}. *Anal.* Found C, 49.15; H, 3.56; N, 4.47%. Calc. for $C_{25}H_{22}N_2PClPt$ (611.96): C, 49.07; H, 3.62; N, 4.58%.

4.9. Diphenylphosphino(phenyl pyridin-2-yl-methylene)amine platinum dimethyl, [PtMe$_2$(**1**-κ^2-P–N)] (**8**)

A Schlenk was charged with **1** (156 mg, 4.26×10^{-4} mol) and $PtMe_2$(COD) (138 mg, 4.14×10^{-4} mol). The solids were stirred, as CH_2Cl_2 (10 mL) was added dropwise. The vessel was sealed and left to stir for 2 days at RT, the initially orange solution stayed orange. The solution was filtered and the solvent removed under reduced pressure to leave **8** as a vivid orange powder, which was washed with hexane (3×10 mL) and dried in vacuo (203 mg, 83%). ^{1}H (301.24 MHz, $CDCl_3$): δ [ppm] = 9.30 (1H, dd + satellites, $^3J_{HH} = 5.7$, $^4J_{PH} = 1.1$, $^3J_{PtH} = 21.9$, C^1*H*), 7.70–7.00 (18H, m, Py*H* + C_6H_5), 0.77 (3H, d + satellites, $^3J_{PH} = 7.9$, $^2J_{PtH} = 65.4$, Pt–C*H*$_3$ {*trans*-P}), 0.53 (3H, d + satellites, $^3J_{PH} = 7.9$, $^2J_{PtH} = 90.6$, Pt–C*H*$_3$ {*cis*-P}). ^{13}C {^{1}H} (75.75 MHz, $CDCl_3$): δ [ppm] = 175.0 (s + satellites, $^3J_{PtC} = 27$, *C*^{6}), 152.5 (s + satellites, $^2J_{PtC} = 14$, *C*^{1}), 147.5 (d, $^3J_{PC} = 14$, *C*^{5}), 139.8 (d, $^3J_{PC} = 14$, *C*^{7}), 137.2 (s, *C*^{3}), 134.2 (d, $^1J_{PC} = 46$, {*i*-C_6H_5}$_2$P), 132.5 (m, {*o*-C_6H_5}$_2$P), 131.8 (s, *C*^{10}), 130.1 (d, $^4J_{PC} = 2$, {*p*-C_6H_5}$_2$P), 129.6 (s, *C*^{8}), 128.4 (s, *C*^{9}), 128.1 (d, $^3J_{PC} = 10$, {*m*-C_6H_5}$_2$P), 127.5 (s + satellites, $^3J_{PtC} = 18$, *C*^{2}), 126.2 (s, *C*^{4}), 10.9 (d + satellites, $^2J_{PC} = 111$, $^1J_{PtC} = 340$, Pt–*C*H$_3$ {*trans*-P}), −21.6 (d + satellites, $^2J_{PC} = 4$, $^1J_{PtC} = 759$, Pt–*C*H$_3$ {*cis*-P}). ^{31}P {^{1}H} (121.94 MHz, $CDCl_3$): δ [ppm] = +65.3 (s + satellites, $^1J_{PtP} = 1259$). MS (FAB$^+$): 576 (M–Me)$^+$, 561 (M–2Me)$^+$. IR (KBr, $CDCl_3$ solution): ν(C=N) = 1605, 1589, 1560 cm^{-1}. *Anal.* Found: C, 52.87; H, 4.18; N, 4.66%. Calc. for $C_{26}H_{25}N_2PPt$ (591.54): C, 52.79; H, 4.26; N, 4.74%.

4.10. Diphenylphosphino(phenyl pyridin-2-yl methylene)-amine methyl acetonitrile palladium (II) tetrakis(3,5-bis(trifluoromethyl)phenyl)borate, [PdMe(MeCN)-(**1**-κ^2-P–N)][B{3,5-(CF$_3$)$_2$-C$_6$H$_3$}$_4$] (**9**)

A Schlenk was charged with **5** (127 mg, 2.42×10^{-4} mol), Na[B{3,5-$(CF_3)_2$-C_6H_3}$_4$] (221 mg, 2.49×10^{-4} mol), acetonitrile (40 mL) and sealed. The vivid yellow solution was stirred at RT for 4 days, then filtered to remove a small amount of white precipitate that had formed. Removal of solvent under reduced pressure left a yellow solid, which was dissolved in CH_2Cl_2 (20 mL) and the solution filtered. Removal of the solvent and drying in vacuo afforded **9** as a vivid yellow solid (296 mg, 91%, m.p. = 70–71 °C).

^{1}H (301.24 MHz, $CDCl_3$): δ [ppm] = 8.68 (1H, dd, $^3J_{HH} = 4.7$, $^4J_{PH} = 0.6$, C^1*H*), 7.64–7.18 (30H, m, Py*H* + C_6H_5 + $C_6H_3(CF_3)_2$), 2.12 (3H, s, C*H*$_3$CN), 0.35 (3H, d, $^3J_{PH} = 2.3$, Pd–C*H*$_3$). ^{13}C {^{1}H} (100.61 MHz, $CDCl_3$): δ [ppm] = 178.5 (d, $^2J_{PC} = 6$, *C*^{6}), 161.9 (q, $^1J_{BC} = 50$, *i*-$C_6H_3(CF_3)_2$), 151.1 (s, *C*^{1}), 148.5 (d, $^3J_{PC} = 16$, *C*^{5}), 139.7 (s, *C*^{3}), 138.2 (d, $^3J_{PC} = 17$, *C*^{7}), 135.0 (br s, *o*-$C_6H_3(CF_3)_2$), 133.8 (s, *C*^{10}), 132.6 (d, $^2J_{PC} = 13$, {*o*-C_6H_5}$_2$P), 132.4 (d, $^4J_{PC} = 3$, {*p*-C_6H_5}$_2$P), 130.4 (d, $^1J_{PC} = 66$, {*i*-C_6H_5}$_2$P), 130.2 (s, *C*^{9}), 129.5 (d, $^3J_{PC} = 11$, {*m*-C_6H_5}$_2$P), 129.4 (m, *m*-$C_6H_3(CF_3)_2$), 129.2 (s, *C*^{8}), 129.3 (d, $^3J_{PC} = 6$, {*m*-C_6H_5}$_2$P), 128.5 (s br, CH$_3$*C*N), 128.3 (s, *C*^{9}), 124.7 (q, $^1J_{FC} = 270$, *C*F$_3$), 119.9 (br, CH$_3$*C*N), 117.7 (m, *p*-$C_6H_3(CF_3)_2$), 2.6 (s, *C*H$_3$CN), 0.7 (s, Pd–*C*H$_3$). ^{31}P {^{1}H} (121.94 MHz, $CDCl_3$): δ [ppm] = +73.7 (s). MS (FAB$^+$): 487 M$^+$, 472 (M–Me)$^+$. MS (FAB$^-$): 863 (B{$C_6H_3(CF_3)_2$}$_4$)$^-$. IR (KBr, $CDCl_3$ solution): ν(C=N) = 1610, 1594 cm^{-1}.

Anal. Found: C, 51.08; H, 2.52; N, 2.95%. Calc. for $C_{59}H_{37}N_3BPF_{24}Pd$ (1392.11): C, 50.90; H, 2.68; N, 3.02%.

4.11. Diphenylphosphino(phenyl pyridin-2-yl methylene)-amine methyl acetonitrile palladium (II) hexafluorophosphate, [PdMe(MeCN)-(**1**-κ^2-P–N)][PF$_6$] (**10**)

A Schlenk was charged with **5** (306 mg, 5.84×10^{-4} mol), $NaPF_6$ (101 mg, 6.01×10^{-4} mol), acetonitrile (60 mL) and sealed. The vivid yellow solution was stirred at RT for 3 days, then filtered to remove the slight white precipitate that had formed. Removal of solvent under reduced pressure left a yellow solid, which was dissolved in CH_2Cl_2 (30 mL) and the solution filtered. Removal of the solvent and drying in vacuo left

10 as a vivid yellow solid (298 mg, 81%, m.p. = 97 °C colour change, yellow to black, 157–158 °C melted).

^{1}H (250.13 MHz, $CDCl_3$): δ [ppm] = 9.37 (1H, br d, $^3J_{HH}$ = 3.5, C^1*H*), 7.77–7.06 (18H, m, Py*H* + C_6H_5), 0.38 (3H, br s, $\nu_{1/2}$ = 6.0 Hz, Pd–C*H*$_3$). ^{13}C {^{1}H} (75.75 MHz, $CDCl_3$): δ [ppm] = 178.1 (d, $^2J_{PC}$ = 6, *C*^{6}), 152.9 (s, *C*^{1}), 147.9 (d, $^3J_{PC}$ = 16, *C*^{5}), 139.3 (s, *C*^{3}), 138.8 (d, $^3J_{PC}$ = 18, *C*^{7}), 133.1 (s, *C*^{10}), 132.6 (d, $^2J_{PC}$ = 12, {*o*-C_6H_5}$_2$P), 131.7 (s, {*p*-C_6H_5}$_2$P), 130.3 (s, *C*^{8}), 129.8 (d, $^1J_{PC}$ = 40, {*i*-C_6H_5}$_2$P), 128.9 (s, *C*^{9}), 128.8 (d, $^3J_{PC}$ = 11, {*m*-C_6H_5}$_2$P), 128.0 (s, *C*^{2}), 127.6 (s, *C*^{4}), 1.2 (s, Pd–*C*H$_3$). ^{31}P {^{1}H} (101.26 MHz, $CDCl_3$): δ [ppm] = +73.4 (br s, $\nu_{1/2}$ = 14.3 Hz, Ph_2P {2-IP}), −144.5 (sept, $^1J_{PF}$ = 716, *P*F$_6$). MS (FAB$^+$): 487 M$^+$, 472 (M–Me)$^+$. MS (FAB$^-$): 145 $(PF_6)^-$. IR (KBr, CH_2Cl_2 solution): ν(C=N) = 1606, 1588, 1564 cm^{-1}.

Anal. Found: C, 47.98; H, 3.60; N, 5.98%. Calc. for $C_{27}H_{25}N_3P_2F_6Pd$ (673.87): C, 48.12; H, 3.74; N, 6.24%.

4.12. Diphenylphosphino(phenyl pyridin-2-yl methylene)-amine η^1-acyl acetonitrile palladium (II) tetrakis(3,5-bis(trifluoromethyl)phenyl)borate, [Pd{C(=O)Me}(MeCN)(**1**-κ^2-P–N)]-[B{3,5-$(CF_3)_2$-C_6H_4}$_4$] (**11**)

A Young's tap NMR tube was charged with **9** (19 mg, 1.36×10^{-5} mol). $CDCl_3$ (0.5 mL) was added, the tube freeze/thaw degassed, then back-filled with CO and sealed. After standing at RT for 6 h, with periodic vigorous shaking, the initially yellow solution became orange.

^{1}H (301.24 MHz, $CDCl_3$): δ [ppm] = 8.73 (1 H, br, C^1*H*), 7.71–7.23 (30H, m, Py*H* + C_6H_5 + $C_6H_3(CF_3)_2$), 2.15 (3H, s, C*H*$_3$CN), 2.03 (3H, d, $^4J_{PH}$ = 1.8, Pd–C(=O)C*H*$_3$). ^{13}C {^{1}H} (75.75 MHz, $CDCl_3$): δ [ppm] = 222.8 (s, Pd–*C*{=O}CH$_3$), 177.6 (d, $^2J_{PC}$ = 6, *C*^{6}), 161.9 (q, $^1J_{BC}$ = 50, *i*-$C_6H_3(CF_3)_2$), 151.1 (s, *C*^{1}), 149.9 (d, $^3J_{PC}$ = 14, *C*^{5}), 139.9 (s, *C*^{3}), 138.2 (d, $^3J_{PC}$ = 18, *C*^{7}), 135.0 (br s, *o*-$C_6H_3(CF_3)_2$), 133.9 (s, *C*^{10}), 132.5 (d, $^4J_{PC}$ = 2, {*p*-C_6H_5}$_2$P), 132.1 (d, $^2J_{PC}$ = 13, {*o*-C_6H_5}$_2$P), 131.20 (d, $^1J_{PC}$ = 60, {*i*-C_6H_5}$_2$P), 130.2 (s, *C*^{8}), 129.5 (d, $^3J_{PC}$ = 11.0, {*m*-C_6H_5}$_2$P), 129.2 (s, *C*^{9}), 129.2 (m, *C*F$_3$), 128.5 (s, *C*^{4}), 127.9 (s, *C*^{2}), 124.7 (q, $^1J_{FC}$ = 273, *C*F$_3$), 119.5 (br, Me*C*N), 117.7 (m, *p*-$C_6H_3(CF_3)_2$), 38.0 (d, $^3J_{PC}$ = 30, Pd–C(=O)*C*H$_3$), 2.5 (s, *C*H$_3$CN). ^{31}P {^{1}H} (101.26 MHz, $CDCl_3$): δ [ppm] = +57.8 (s). MS (FAB$^+$): 515 (M–CH_3CN)$^+$, 472 (M–CH_3CN-acyl)$^+$. MS (FAB$^-$): 863 (B{$C_6H_3(CF_3)_2$}$_4$)$^-$. R (KBr, CH_2Cl_2 solution): ν(C=O) = 1653 cm^{-1}; ν(C=N) = 1610, 1590 cm^{-1}.

4.13. Diphenylphosphino(phenyl pyridin-2-yl methylene)-amine palladium η^1-acyl chloride, [PdCl{η^1-C(=O)Me}(**1**-κ^2-P–N)] (**12**)

A thick-walled Young's tap NMR tube was charged with **5** (51 mg, 9.75×10^{-5} mol). $CDCl_3$ (0.5 mL) was added, the tube freeze/thaw degassed, then back-filled with CO and sealed. After standing at RT for 2 days, with periodic vigorous shaking, the initially yellow solution became bright red. ^{1}H NMR (301.24 MHz, $CDCl_3$): δ [ppm] = 9.54 (1H, dd, $^3J_{HH}$ = 5.0, $^4J_{PH}$ = 1.1, C^1*H*), 7.69–7.21 (17H, m, Py*H* + C_6H_5), 7.08 (1H, d, $^3J_{HH}$ = 7.9, C*H*), 2.04 (3H, d, $^4J_{PH}$ = 1.7, Pd–C{=O}C*H*$_3$). ^{13}C {^{1}H} NMR (75.75 MHz, $CDCl_3$): δ [ppm] = 227.0 (d, $^2J_{PC}$ = 9, Pd–*C*{=O}CH$_3$), 176.3 (d, $^2J_{PC}$ = 3, *C*^{6}), 153.3 (s, *C*^{1}), 149.3 (d, $^3J_{PC}$ = 13, *C*^{5}), 139.4 (d, $^3J_{PC}$ = 16, *C*^{7}), 138.5 (s, *C*^{3}), 133.6 (d, $^1J_{PC}$ = 55, {*i*-C_6H_5}$_2$P), 132.7 (s, *C*^{10}), 132.1 (d, $^2J_{PC}$ = 14, {*o*-C_6H_5}$_2$P), 131.3 (d, $^4J_{PC}$ = 2, {*p*-C_6H_5}$_2$P), 130.1 (s, *C*^{8}), 128.9 (s, *C*^{9}), 128.7 (d, $^3J_{PC}$ = 4, {*m*-C_6H_5}$_2$P), 127.5 (s, *C*^{2}), 127.1 (s, *C*^{4}), 39.00 (d, $^3J_{PC}$ = 25, Pd–C{=O}*C*H$_3$). ^{31}P {^{1}H} NMR (121.94 MHz, $CDCl_3$): δ [ppm] = +56.1 (s). MS (FAB$^+$): 515 (M–Cl)$^+$, 507 (M-acyl)$^+$, 487 (M–Cl-Me)$^+$, 472 (M–Cl-acyl)$^+$. IR (KBr, $CDCl_3$ solution): ν(C=O) = 1696 cm^{-1}; ν(C=N) = 1610, 1588, 1565 cm^{-1}.

4.14. Reaction of [PdCl{C(=O)Me}(**1**-κ^2-P–N)] (**12**) with CH_2=CH_2, formation of **13**

In a thick-walled Young's tap NMR tube, a $CDCl_3$ (0.5 mL) solution of **7** (6 mg, 1.09×10^{-5} mol) prepared as previously described, was freeze/thaw degassed, back-filled with CH_2=CH_2 and sealed. After standing at RT for 3 days, no reaction was evident by ^{31}P {^{1}H} NMR spectroscopy. After raising the pressure of CH_2=CH_2 in the tube to ~10 atmospheres, ^{1}H and ^{31}P {^{1}H} NMR spectroscopies showed a new peak corresponding to the product resulting from insertion (within 10 min of CH_2=CH_2 being added), in addition to a peak for the acyl starting material, in a 1:1 ratio. Standing at RT for 18 h caused no change according to ^{1}H and ^{31}P {^{1}H} NMR spectroscopies. ^{31}P {^{1}H} NMR (101.26 MHz, $CDCl_3$): δ [ppm] = +72.1 (s, **13**), +56.1 (s, **12**).

Data for complex **13** only: ^{1}H NMR (250.13 MHz, $CDCl_3$): δ [ppm] = 9.66 (1H, dd, $^3J_{HH}$ = 5.0, $^4J_{PH}$ = 0.9, C^1*H*), 7.71–7.19 (18H, m, Py*H* + C_6H_5), 2.30 (2H, pseudo-td, $^3J_{HH}$ = 8.2, $^4J_{PH}$ = 3.2, Pd–CH_2–C*H*$_2$–C{=O}CH$_3$), 1.70 (3H, s, Pd–CH_2–CH_2–C{=O}C*H*$_3$), 1.54 (2H, m, Pd–C*H*$_2$–CH_2–C{=O}CH$_3$).

4.15. Diphenylphosphino(phenyl pyridin-2-yl-methylene)amine palladium N-tert-butyl-η^1-iminoacyl-chloride, [PdCl{η^1-C(=NBu^t)Me}(**1**-κ^2-P–N)] (**14**)

A Young's tap NMR tube was charged with **12** (15 mg, 2.87×10^{-5} mol). $CDCl_3$ (0.5 mL) was added and the tube freeze/thaw degassed. Bu^{t}NC (2.87×10^{-5} mol) was then added via vacuum transfer using a gas/vapour addition bulb and Hg manometer, the tube back-filled with N_2 and sealed. After standing

at RT for 1 h the initially yellow solution turned deep red. ^{1}H NMR (250.13 MHz, $CDCl_3$): δ [ppm] = 9.84 (1H, dd, $^3J_{HH}$ = 5.6, $^4J_{PH}$ = 1.0, C^1*H*), 7.96–7.21 (18H, m, Py*H* + C_6H_5), 2.85 (3H, d, $^4J_{PH}$ = 2.1, Pd–C{=NC$(CH_3)_3$}C*H*$_3$), 1.43 (9H, s, Pd–C{=NC-(C*H*$_3)_3$}CH_3). ^{13}C {^{1}H} NMR (75.75 MHz, $CDCl_3$): δ [ppm] = 179.5 (d, $^2J_{PC}$ = 4, *C*^{6}), 154.8 (s, *C*^{1}), 148.9 (d, $^2J_{PC}$ = 24, Pd–*C*{=NC$(CH_3)_3$}CH_3), 147.0 (d, $^3J_{PC}$ = 18.0, *C*^{5}), 140.4 (s, *C*^{3}), 138.0 (d, $^3J_{PC}$ = 18.0, *C*^{7}), 133.9 (s, *C*^{10}), 133.23 (d, $^4J_{PC}$ = 3, {*p*-C_6H_5}$_2$P), 132.8 (d, $^2J_{PC}$ = 13, {*o*-C_6H_5}$_2$P), 131.5 (d, $^3J_{PC}$ = 12, {*m*-C_6H_5}$_2$P), 130.5 (s, *C*^{8}), 129.2 (s, *C*^{9}), 128.4 (s, *C*^{2}), 128.3 (s, *C*^{4}), 60.0 (s, Pd–C{=N*C*$(CH_3)_3$}CH_3), 34.9 (d, $^3J_{PC}$ = 4, Pd–C{=NC$(CH_3)_3$}*C*H$_3$), 29.2 (s, Pd–C{=NC(*C*H$_3)_3$}CH_3). {*i*-C_6H_5}$_2$P was not observed. ^{31}P {^{1}H} NMR (101.26 MHz, $CDCl_3$): δ [ppm] = +57.9 (s). MS (FAB$^+$): 606 $(MH)^+$, 570 $(M–Cl)^+$, 473 (M–Cl–C{=NC$(CH_3)_3$}$CH_3)^+$. IR (KBr, CH_2Cl_2 solution): 1593 (C=N) cm^{-1}.

4.16. X-Ray crystal structure analyses

X-ray diffraction data (Table 5) were collected on a Bruker Apex 2K CCD area detector diffractometer equipped with an Oxford Cryostream N_2 cooling device, using graphite monochromated Mo-K_α X-radiation (λ = 0.71073 Å). Data collection and reduction were conducted using the SMART and SAINT programs [77], respectively. All further calculations were performed using the SHELXTL package [78] and programs therein. Structures were solved using Patterson methods. All structures were refined using full-matrix least squares based on F^2. An empirical absorption correction was applied to all data using SADABS [79]. All non-hydrogen atoms were refined anisotropically, then hydrogen atoms included at idealised positions and refined as rigid groups.

4.17. Catalytic testing

Catalyst testing was undertaken in a custom-made HEL Automate autoclave system (stainless steel) under computer control. Stirring was achieved using a magnetically driven paddle stirrer. Temperature control was achieved using both an internal heater coil and an external heater jacket and monitored both inside and out. Autoclave dried under flow of N_2 at elevated temperature. Procatalysts were introduced into the autoclave quickly under air and the system rapidly purged with nitrogen. Solvent (dry MeOH) was added to the reaction

Table 5
Crystallographic data for the complexes **3**, **4**, **6**, and **7**

Complex	**3** · $CDCl_3$	**4** · CD_2Cl_2	**6** · CH_2Cl_2	**7**
Empirical formula	$C_{25}H_{19}N_2OPClRh \cdot CDCl_3$	$C_{24}H_{19}N_2PCl_2Pd \cdot CD_2Cl_2$	$C_{24}H_{19}N_2PCl_2Pt \cdot CH_2Cl_2$	$C_{25}H_{22}N_2PClPt$
Formula weight	653.13	630.62	717.30	611.96
Temperature (K)	150(2)	150(2)	150(2)	150(2)
Crystal system	Monoclinic	Triclinic	Monoclinic	Orthorhombic
Space group	*P*2(1)/*n*	$P\bar{1}$	*P*2(1)/*n*	*P*2(1)2(1)2(1)
a (Å)	12.9589(5)	9.0218(4)	12.5494(6)	9.6133(4)
b (Å)	12.2356(4)	10.8340(5)	12.3151(6)	12.0936(4)
c (Å)	17.8924(6)	14.3981(7)	17.6121(8)	20.3218(7)
α (°)	90	75.3150(10)	90	90
β (°)	102.035(1)	83.4430(10)	100.8050(10)	90
γ (°)	90	68.9620(10)	90	90
Volume (Å^3)	2774.66(17)	1270.17(10)	2673.6(2)	2362.60(15)
Z	4	2	4	4
D_{calc} (mg/m^3)	1.563	1.649	1.782	1.720
Absorption coefficient (mm^{-1})	1.081	1.232	5.724	6.134
Crystal size (mm^3)	0.42 × 0.37 × 0.34	0.34 × 0.30 × 0.14	0.340.28 × 0.26	0.39 × 0.24 × 0.21
θ-range (°)	1.78 to 26.00	1.46 to 26.00	1.84 to 27.00	1.96 to 28.00
Reflections collected	21045	9969	22078	20653
Independent reflections	5437	4929	5843	5577
	[$R_{(int)}$ = 0.0155]	[$R_{(int)}$ = 0.0146]	[$R_{(int)}$ = 0.0289]	[$R_{(int)}$ = 0.0423]
Completeness to θ	26.00°/99.9%	26.00°/98.9%	27.00°/100.0%	28.00°/99.1%
Absorption correction	Empirical	Empirical	Empirical	Empirical
Maximum and minimum transmission	0.86 and 0.75	0.93 and 0.76	0.86 and 0.50	0.75 and 0.34
Data/restraints/parameters	5437/0/316	4929/0/298	5843/0/298	5577/0/272
Goodness-of-fit on F^2	1.044	1.047	1.146	1.020
Final *R* indices [$I > 2\sigma(I)$]	R_1 = 0.0251	R_1 = 0.0214	R_1 = 0.0324	R_1 = 0.0216
	wR_2 = 0.0672	wR_2 = 0.0576	wR_2 = 0.1049	wR_2 = 0.0465
R indices (all data)	R_1 = 0.0267	R_1 = 0.0227	R_1 = 0.0341	R_1 = 0.0224
	wR_2 = 0.0680	wR_2 = 0.0582	wR_2 = 0.1056	wR_2 = 0.0467
Absolute structure parameter	–	–	–	0.002(5)
Largest differential peak and hole (e Å^{-3})	1.103 and −0.999	0.463 and −0.637	3.136 and −1.289	1.121 and −0.778

Standard deviations are given in parentheses.

vessel via syringe under a flow of nitrogen. Where appropriate, activator ($MeSO_3H$) was also added via syringe under a flow of nitrogen. The reactor vessel was saturated with $CO:C_2H_4$ (1:1, 38 bar) at ambient temperature prior to rapid warming of the vessel to the desired reaction temperature.

At the end of a run, the CO/C_2H_4 feedstock was replaced by nitrogen and the reactor cooled to ambient temperature. The organic phase was separated by filtration. The crude mixture was subject to GC–MS analysis prior to removal of all volatiles under reduced pressure and isolation of the carbonylation product.

4-Oxo-hexanoic acid methyl ester (**15**): ^{13}C $\{^1H\}$ NMR (75.75 MHz, $CDCl_3$): δ [ppm] = 208.6 (s, $CH_3CH_2C(O)CH_2$), 177.7 (s, $C(O)OCH_3$), 52.2 (s, OCH_3), 36.8 (s, $CH_3CH_2C(O)CH_2$), 36.2 (s, CH_3CH_2-$C(O)CH_2$), 28.1 ($CH_2C(O)OCH_3$), 8.1 (s, CH_3CH_2). GC–MS: 144 (M^+, 7.68 min).

5. Supplementary material

Crystallographic data for the structural analyses have been deposited with the Cambridge Crystallographic Data Centre, CCDC, Nos. CCDC 261271–261274 for **3**, **4**, **6**, and **7**, respectively. Copies of this information may be obtained free of charge from The Director, 12 Union Road, Cambridge, CB2 1EZ, UK (fax: +44 1223 336 033: e-mail deposit@ccdc.cam.ac.uk or www: http://www.ccdc.cam.ac.uk).

Acknowledgements

The Royal Society and The Nuffield Foundation are thanked for grants to PWD. Johnson Matthey Plc. is thanked for the loan of platinum group metal salts. Financial support from the EPSRC (PWD {JREI GR/R05802/01}, MJH), Lubrizol Ltd. (CASE award MJH), and The University of Leicester is gratefully acknowledged. Dr. G. Griffith is thanked for his assistance with the acquisition of non-routine NMR spectra.

References

[1] (a) P. Braunstein, F. Naud, Angew. Chem. Int. Ed. 40 (2001) 680;
(b) P.J. Guiry, C.P. Saunders, Adv. Synth. Catal. 346 (2004) 497;
(c) W.J. Drury III, N. Zimmermann, M. Keenan, M. Hayashi, S. Kaiser, R. Goddard, A. Pfaltz, Angew. Chem. Int. Ed. Engl. 43 (2004) 70;
(d) F. Leca, C. Lescop, R. Réau, Organometallics 23 (2004) 6191;
(e) C. Bianchini, A. Meli, Coord. Chem. Rev. 225 (2002) 35;
(f) P. Espinet, K. Soulantica, Coord. Chem. Rev. 193–195 (1999) 499.

[2] D.J. Cole-Hamilton, R.A.M. Robertson, in: A. Sen (Ed.), Catalytic Synthesis of Alkene-carbon Monoxide Copolymers and Cooligomers, Kluwer Academic Publishers, Dordrecht, 2003, pp. 37–82 (Chapter 3).

[3] R.A.M. Robertson, D.J. Cole-Hamilton, Coord. Chem. Rev. 225 (2002) 67.

[4] M. Beller, A.M. Tafesh, in: B. Cornils, W.A. Herrmann (Eds.), Applied Homogeneous Catalysis with Organometallic Compounds, Wiley–VCH, Weinheim, 2002, pp. 182–194.

[5] D. Milstein, Acc. Chem. Rev. 21 (1988) 428.

[6] A. Baceiredo, G. Bertrand, P.W. Dyer, J. Fawcett, N. Griep-Raming, O. Guerret, M.J. Hanton, A.-M. Williamson, New J. Chem. 25 (2001) 591.

[7] F. Dahan, P.W. Dyer, M.J. Hanton, M. Jones, D.M.P. Mingos, A.J.P. White, D.J. Williams, A.-M. Williamson, Eur. J. Inorg. Chem. (2002) 732.

[8] P.W. Dyer, J. Fawcett, M.J. Hanton, R.D.W. Kemmitt, R. Padda, D.R. Russell, N. Singh, J. Chem. Soc. Dalton Trans. (2003) 104.

[9] M.L. Clarke, G.L. Holliday, A.M.Z. Slawin, J.D. Woollins, J. Chem. Soc., Dalton Trans (2002) 1093.

[10] M. Rodriguez i Zubiri, J.D. Woollins, Comm. Inorg. Chem. 24 (2003) 189.

[11] M. Brookhart, S.D. Ittel, L.K. Johnson, Chem. Rev. 100 (2000) 1169.

[12] B. Cornils, W.A. Herrmann (Eds.), Applied Homogeneous Catalysis with Organometallic Compounds, vol. 1, Second ed., Wiley–VCH, Weinheim, 2002 (Chapters 2.1, 2.2 and 2.3).

[13] K.R. Reddy, K. Surekha, G.-H. Lee, S.-H. Peng, J.-T. Chen, S.-T. Liu, Organometallics 20 (2001) 1292.

[14] S.M. Aucott, A.M.Z. Slawin, J.D. Woollins, J. Organomet. Chem. 582 (1999) 83.

[15] L. Canovese, G. Chessa, L. Maini, M. Polito, C. Santo, P. Uguagliati, F. Visentin, J. Chem. Soc., Dalton Trans. (2002) 3696.

[16] I. Fleming, D.H. Williams, Spectroscopic Methods in Organic Chemistry, fourth ed., McGraw Hill, London, 1987, p. 91–92.

[17] (a) N.G. Anderson, B.A. Keay, Chem. Rev. 101 (2001) 997;
(b) C. Glidewell, E.J. Leslie, J.C.S. Dalton Trans. (1977) 527;
(c) D.W. Allen, B.F. Taylor, J. Chem. Res. (S) (1981) 220;
(d) R.D. Kroshefsky, R. Weiss, J.G. Verkade, Inorg. Chem. 18 (1979) 469;
(e) D.W. Allen, B.R. Taylor, J. Chem. Soc. Dalton Trans. (1982) 51.

[18] R.G. Pearson, Inorg. Chem. 12 (1973) 712.

[19] M.P. Anderson, A.L. Casalnuovo, B.J. Johnson, B.M. Mattson, A.M. Mueting, L.H. Pignolet, Inorg. Chem. 27 (1988) 1649.

[20] Y. Arikawa, M. Hidai, Y. Nishibayashi, K. Ohe, K. Segawa, S. Uemura, J. Organomet. Chem. 545 (1997) 381.

[21] A.D. Burrows, M.F. Mahon, M. Varrone, Dalton Trans. (2003) 4718.

[22] S. Vastag, B. Heil, L. Markü, J. Mol. Catal. 5 (1979) 189.

[23] P.H.M. Budzelaar, E. Drent, Chem. Rev. 96 (1996) 663.

[24] S.M. Aucott, A.M.Z. Slawin, J.D. Woollins, J. Chem. Soc. Dalton Trans. (2001) 2279.

[25] C.J. Cobley, P.G. Pringle, Inorg. Chim. Acta 265 (1997) 107.

[26] G.P.C.M. Dekker, C.J. Elsevier, P.W.N.M. van Leeuwen, K. Vrieze, Organometallics 11 (1992) 1598.

[27] J. Boersma, W. de Graaf, G. van Koten, W.J.J. Smeets, A.L. Spek, Organometallics 8 (1989) 2907.

[28] J. Boersma, W. de Graaf, S. Harder, J.A. Kanters, G. van Koten, J. Organomet. Chem. 358 (1988) 545.

[29] G.J. Palenik, W.L. Steffen, Inorg. Chem. 15 (1976) 2432.

[30] P–N single bond lengths: 1.77 Å, in: N.N. Greenwood, A. Earnshaw, Chemistry of the Elements, 1st ed., Butterworth Heinemann, Oxford, 1984, p. 620; 1.8 Å, in: A.L. Pauling, Nature of the Chemical Bond, Cornell University Press, New York, 1960; 1.76 Å: in V. Schomaker and D.P. Stevenson, J. Am. Chem. Soc. 63 (1941) 37.

[31] J. March, Advanced Organic Chemistry, fourth ed., Wiley–Interscience, New York, 1992, p. 21.
[32] P.S. Pregosin, R.W. Kunz, in: P. Diehl, E. Fluck, R. Kosfeld (Eds.), ^{31}P and ^{13}C NMR of Transition Metal Phosphine Complexes, Springer-Verlag, New York, 1979, p. 114.
[33] (a) H. Kobayashi, H. Nishida, T. Sonoda, N. Takada, M. Yoshimura, Bull. Chem. Soc. Jpn. 57 (1984) 2600;
(b) G.J.P. Britovsek, V.C. Gibson, D.F. Wass, Angew. Chem. Int. Ed. 38 (1999) 428;
(c) M. Brookhart, B. Grant, A.F. Volpe, Organometallics 11 (1992) 3920.
[34] C.-L. Chen, J.-T. Chen, S.-T. Liu, Y.-H. Liu, S.-M. Peng, K.R. Reddy, Organometallics 18 (1999) 2574.
[35] A. Buijs, G.P.C.M. Dekker, C.J. Elsevier, P.W.N.M. van Leeuwen, W.J.J. Smeets, A.L. Spek, C.H. Stam, K. Vrieze, Y.F. Wang, Organometallics 11 (1992) 1937.
[36] L.D. Durfee, I.P. Rothwell, Chem. Rev. 88 (1988) 1059.
[37] J.J. Alexander, E.J. Kuhlmann, Coord. Chem. Rev. 33 (1980) 195.
[38] R.E. Rülke, J.G.P. Delis, A.M. Groot, C.J. Elsevier, P.W.N.M. van Leeuwen, K. Vrieze, K. Goubitz, H. Schenk, J. Organomet. Chem. 508 (1996) 109.
[39] P.H.P. Brinkman, G.A. Luinstra, J. Organomet. Chem. 572 (1999) 193.
[40] A. Sommazzi, F. Garbassi, Prog. Polym. Sci. 22 (1997) 1547.
[41] P. Braunstein, C. Frison, X. Morise, Angew. Chem. Int. Ed. 39 (2000) 2867.
[42] J. Boersma, H. Kooijman, G. van Koten, D. Kruis, M. Lakin, B.A. Markies, M.H.P. Rietveld, A.L. Spek, K.A.N. Verkerk, J. Am. Chem. Soc. 117 (1995) 5263.
[43] J. Brumbaugh, M. Parvez, A. Sen, R.R. Whittle, Organometallics 9 (1990) 1735.
[44] J.S. Brumbaugh, A. Sen, J. Am. Chem. Soc. 110 (1988) 803.
[45] C. Bianchini, A. Meli, W. Oberhauser, Dalton Trans. (2003) 2627.
[46] J.P. Collman, R.G. Finke, L.S. Hegedus, J.R. Norton, Principles and Applications of Organotransition Metal Chemistry, University Science Books, Mill Valley, CA, 1987, p. 377–378.
[47] C. Elschenbroich, A. Salzer, Organometallics – a Concise Introduction, second ed., VCH, Weinheim, 1992, p. 240–241.
[48] (a) P.G. Aubel, J.G.P. Delis, P.W.N.M. van Leeuwen, A.L. Spek, N. Veldman, K. Vrieze, J. Chem. Soc., Chem. Commun. (1995) 2233;
(b) P.G. Aubel, J.G.P. Delis, P.W.N.M. van Leeuwen, F.J.R. van Neer, A.L. Spek, N. Veldman, K. Vrieze, Organometallics 16 (1997) 2948.
[49] D.G. Cooper, J. Powell, Can. J. Chem. 51 (1973) 1634.
[50] J.H. Nelson, D.A. Redfield, Inorg. Chem. 12 (1973) 15.
[51] (a) B. Milani, A. Scarel, G. Mestroni, S. Gladiali, R. Taras, C. Carfagna, L. Mosca, Organometallics 21 (2002) 4965;
(b) C. Carfagna, S. Gladiali, G. Mestroni, B. Milani, L. Mosca, A. Scarel, R. Taras, Organometallics 21 (2002) 1323.
[52] B.A. Markies, D. Kruis, M.H.P. Rietveld, K.A.N. Verkerk, J. Boersma, H. Kooijman, M.T. Lakin, A.L. Spek, G. van Koten, J. Am. Chem. Soc. 117 (1995) 5263.
[53] C.S. Schultz, J. Ledford, J.M. DeSimone, M. Brookhart, J. Am. Chem. Soc. 122 (2000) 6351.
[54] C. Bianchini, A. Meli, G. Müller, W. Oberhauser, E. Passaglia, Organometallics 21 (2002) 4965.
[55] P. Champkin, W. Clegg, S. Doherty, M.R.J. Elsegood, G.R. Eastham, A. Harriamn, J.G. Knight, M. Betham, E.G. Robins, R.P. Tooze, Organometallics 19 (2000) 4957.
[56] K.S. Coleman, A.R. Cowley, M.L.H. Green, S.I. Pascu, N.H. Rees, L.H. Rees, J. Chem. Soc., Dalton Trans. (2001) 3384.
[57] P. Braunstein, M.D. Fryzuk, M. Le Dall, F. Naud, S.J. Rettig, F. Speiser, J. Chem. Soc. Dalton Trans. (2000) 1067.
[58] J.-T. Chen, G.-H. Lee, S.-T. Liu, S.-M. Peng, K.R. Reddy, K. Surekha, W.-W. Tsai, J. Chem. Soc., Dalton Trans. (2002) 1776.
[59] E.K. van den Beuken, W.J.J. Smeets, A.L. Spek, B.L. Feringa, Chem. Commun. (1998) 223.
[60] P.H.P. Brinkman, G.A. Luinstra, Organometallics 17 (1998) 5160.
[61] P.W.N.M. van Leeuwen, M.A. Zuideveld, B.H.G. Swennenhuis, Z. Freixa, P.C.J. Kamer, K. Goubitz, J. Fraanje, M. Lutz, A.L. Spek, J. Am. Chem. Soc. 125 (2003) 5523.
[62] G. Cavinato, L. Toniolo, J. Organomet. Chem. 398 (1990) 187.
[63] W.P. Mul, A.W. van der Made, A.A. Smaardijk, E. Drent, in: A. Sen (Ed.), Drent in Catalytic Synthesis of Alkene-carbon Monoxide Copolymers and Cooligomers, Kluwer Academic Publishers, Dordrecht, 2003, pp. 77–140, Ch. 4.
[64] Z. Freixa, P.W.N.M. van Leeuwen, Dalton Trans. (2003) 1890.
[65] P.W.N.M. van Leeuwen, in: A. Sen (Ed.), Catalytic Synthesis of Alkene-carbon Monoxide Copolymers and Cooligomers, Kluwer Academic Publishers, Dordrecht, 2003, pp. 77–173, 184.
[66] W. Clegg, G.R. Eastham, M.R.J. Elsegood, R.P. Tooze, X.L. Wang, K. Whiston, Chem. Commun. (1999) 1877.
[67] E. Drent, J.A.M. Vanbroekhoven, M.J. Doyle, J. Organomet. Chem. 417 (1991) 235.
[68] D.J. Darensbourg, R.L. Kump, Inorg. Chem. 17 (1978) 2680.
[69] J.A. McCleverty, G. Wilkinson, Inorg. Synth. 8 (1966) 211.
[70] S. Komiya, Synthesis of Organometallic Compounds – a Practical Guide, Wiley–Interscience, New York, 1998, p. 285.
[71] C.J. Elsevier, J.M. Ernsting, P.W.N.M. van Leeuwen, R.E. Rulke, A.L. Spek, K. Vrieze, Inorg. Chem. 32 (1993) 5769.
[72] J. Boersma, W. de Graaf, D. Grove, G. van Koten, A.L. Spek, Rec. Trav. Chim. Pays Bas 107 (1988) 299.
[73] J.X. McDermott, J.F. White, G.M. Whitesides, J. Am. Chem. Soc. 98 (1976) 6521.
[74] G.P.C. Dekker, A. Buijs, C.J. Elsevier, P.W.N.M. van Leeuwen, W.J.J. Smeets, A.L. Spek, C.J. Stam, K. Vrieze, Y.F. Wang, Organometallics 11 (1992) 1937.
[75] E. Costa, P.G. Pringle, M. Ravetz, Inorg. Synth. 31 (1997) 284.
[76] H. Kobayashi, H. Nishida, T. Sonoda, N. Takada, M. Yoshimura, Bull. Chem. Soc. Jpn. 57 (1984) 2600.
[77] Bruker SMART (v 5.622, 2001) and SAINT-Plus (v 6.02, 1999), Bruker AXS Inc., Madison, WI, USA.
[78] G.M. Sheldrick, SHELXTL (v 6.1, 2000), Bruker AXS Inc., Madison, WI, USA, 2000.
[79] G.M. Sheldrick, SADABS, Program for the Empirical Absorption Correction of Area Detector Data, University of Göttingen, Germany, 1996.